Detailed response to the Reviewers' comments

We are very grateful for the constructive and helpful comments we received from both reviewers. Accounting for them has been of great help to improve the manuscript.

Referee #1:

General Comments: Waelbroeck et al. present results for 2 cores from the North Brazilian margin, using proxies for AMOC-related ocean circulation changes (Pa/Th, C. wuellerstorfi d13C) and South American precipitation events (Ti/Ca). As the proxy records were generated from the same location/core (more or less) the authors argue that there are no lead/lags related to age model uncertainty and hence this allows to properly assess the phase relationship between AMOC and South American rainfall during the last 45 kyr. Their new data allows to not only focus on the last 4 Heinrich stadials (already presented in Burckel et al., 2015), but also D-O events with shorter frequencies. Based on the careful analysis of their data (using mainly cross-wavelet analyses), they infer that changes in water mass transport in the mid-depth range of the western equatorial Atlantic precede precipitation changes in Brazil. This is especially the case at Heinrich-like frequencies, and less so at D-O frequencies, which they relate to a positive feedback mechanism in the ocean/atmosphere system during Heinrich stadials.

The manuscript is well written, well structured, and concerns an important topic that is certainly relevant for Climate of the Past. In essence, this paper is an evolution of the Burckel et al. (2015) paper, but with some extra Pa/Th and d13C data, which makes it possible to better study changes in water mass transport over Dansgaard-Oeschger frequencies. In general, the authors carefully address the possible biases on Pa/Th and other proxy records (influences by marine productivity, differential bioturbation, currents etc.) and deliver quite a good case for the ocean circulation changes and leads/lags to South American precipitation during D-O/Heinrich stadials. I do have some reservations about the age model, as I think there are some details missing in text to properly evaluate the chronology (and uncertainty). Moreover, more details on some of the geochemical analyses are required (citing an "in prep." paper is in my opinion not enough). If these two main issues are properly addressed, I certainly recommend publication in Climate of the Past.

We have added all the requested information concerning the age model and isotopic analyses in the material and methods section, as described in details below.

Specific Comments: p.2 line 18: XRF, do you mean XRF core scanning (as in Jaeschke et al., 2007, done with the CORTEX scanner) or with more conventional XRF done on glass beads/pressed tablets? If it is the former, please change the abbreviation throughout the text, e.g., XRF-core-scanning (XCS).

We mean XRF core scanning, as in Jaeschke et al. (2007). The XRF data of core MD09-3257 were produced with an AVAATECH XRF core scanner, as now described in the material and methods section of the article. We prefer to keep the abbreviation XRF throughout the text though because this is the abbreviation commonly used and the abbreviation most easily understandable by the reader since it directly refers to the physical principal behind the measurement technique. Moreover, we use the GeoB3910 XRF data from Jaeschke et al. (2007), who used the denomination XRF throughout their paper. Also, thanks to the new paragraph describing the measurement method, there can be no confusion any longer.

p. 3, line 9: I miss a paragraph on the geochemical measurements performed to derive the Ti/Ca ratio. The Ti/Ca values were already published in Burckel et al. (2015), but I cannot find the XRF methods in there (I could have overlooked it). The best would be to give details on the used methods here, at least briefly. Note also that if you used the same method as Jaeschke et al. (2007), you probably used a different core scanner (Avaatech? Itrax?).

We thank Referee 1 for having identified this omission in the submitted version of our article. We have added the following paragraph to the material and methods section:

"***X-Ray Fluorescence Spectrometry***

Elemental composition was measured employing nondestructive, profiling X-ray fluorescence (XRF) spectrometry. The measurements were made using an AVAATECH XRF Core Scanner at the Bjerkness Centre for Climate Research, Bergen (Norway) at intervals of 0.5 mm on core MD09-3257, and using a CORTEX XRF Scanner at the Bremen Integrated Ocean Drilling Program core repository at intervals of 0.4 cm on core GeoB3910-2 (Jaeschke et al., 2007). This automated scanning method allows for a rapid qualitative determination of the geochemical composition of the sediment at very high resolution (Croudace and Rothwell, 2015)."

p.3, line 22: Log-ratios of Ti/Ca are indeed the way to go, also, because they allow a better statistical modelling of compositional data (see Weltje and Tjallingii, 2008; normal ratios are asymmetric). It would be good to shortly address this too in this sentence.

We thank Referee 1 for his/her remark and for his/her recommendation to read the article Weltje and Tjallingii (2008), which we found very informative. We have changed the sentence

"Here, we use XRF ln(Ti/Ca) rather than Ti/Ca because small precipitation events are more clearly marked in ln(Ti/Ca) than in Ti/Ca."

into

"Here, we use XRF ln(Ti/Ca) rather than Ti/Ca because log-ratios provide a unique measure of sediment composition, in contrast to simple ratios, which are asymmetric (i.e. conclusions based on evaluation of A/B cannot be directly translated into equivalent statements about B/A) and hence suffer from statistical intractability (Weltje and Tjallingii, 2008)."

p.3, lines 9-27 (Chronology): I find the chronological section not yet satisfying. For instance, I miss what software was used to calculate the age model (OxCal?), and more technical details (reservoir age? uncertainties?). I see that in Burckel et al. (2015) the age model is addressed in one of the 16 Supplements of that paper, but I think it is important to at least briefly address the most important parts again. As written now, you might as well have used a simple linear model between the age points, but I cannot find that in the text. As the age model is clearly crucial for the results of this paper, the details should be better outlined (and not simply covered by a reference to an "in prep." paper). For instance, did the authors use the state-of-the-art OxCal Bayesian modeling, and if not, why not? The authors should read the Sections 3 and 4 in the Supplement of Grant et al. (2012), who do a good job of obtaining the chronological uncertainties with a Bayesian deposition model in OxCal (also to calculate lags/leads between proxy records, albeit with a different scope).

All radiocarbon dates were converted to calendar dates using the OxCal 4.2 software, the IntCal13 calibration curve, and a surface water reservoir age of 550 ± 50 y between 0 – 18 ka

(Key et al., 2004), and of 750 ± 250 y between 18 – 31 ka (Freeman et al., 2016). The final age models were obtained using the state-of-the-art OxCal Bayesian modeling. We have added the age uncertainty for each core depth in Table S1 and S2.

The article (Vazquez Riveiros et al., in prep.) is unfortunately not accepted yet. We have thus added all the information requested by Referee 1 to the section describing the chronology of our cores. The following sentences have been added:

"The chronology of core GeoB3910-2 is based on 17 monospecific radiocarbon dates between 0 and 31 ka (Burckel et al., 2015; Jaeschke et al., 2007). The Ti/Ca record of core GeoB3910-2 was aligned to that of core MD09-3257 in order to transfer the radiocarbon dates of GeoB3910-2 over the interval 12–36 ka to this nearby core. In addition, five monospecific radiocarbon dates over 1–21 ka were obtained directly on core MD09-3257. Speleothem tie points were used to derive the chronology of this core over 38–48 ka (Table S1 and S2) (Vazquez Riveiros et al., submitted). All radiocarbon dates were converted to calendar dates using the OxCal 4.2 software, the IntCal13 calibration curve (Reimer et al., 2013), and a surface water reservoir age of 550 ± 50 y over 0–18 ka (Key et al., 2004), and of 750 ± 250 y over 18–31 ka (Freeman et al., 2016). The final age models of cores GeoB3910-2 and MD09-3257 were obtained using a *P_Sequence* depositional model (Bronk Ramsey, 2008), i.e. a Bayesian algorithm producing posterior probability distributions for each core depth (Table S1 and S2) (Vazquez Riveiros et al., submitted)."

p.4, lines 1-16: The details on the d13C methods should be given here, and not in the Vazquez Riveiros (in prep.) paper.

We have added the requested information to the material and methods section:

"Epifaunal benthic foraminifers of the *Cibicides wuellerstorfi* species were handpicked in the >150 mm size fraction (Vazquez Riveiros et al., submitted). Core MD09-3257 *C. wuellerstorfi* $^{13}C/^{12}C$ ($\delta^{13}C$, expressed in ‰ versus Vienna Pee-Dee Belemnite, VPDB) was measured at the LSCE on Finnigan Δ+ and Elementar Isoprime mass spectrometers on samples of 1 to 3 specimens. VPDB is defined with respect to the NBS-19 calcite standard ($\delta^{18}O$ = -2.20 ‰ and $\delta^{13}C$ = +1.95 ‰). The mean external reproducibility (1σ) of carbonate standards is ± 0.03 ‰ for $\delta^{13}C$; measured NBS-18 $\delta^{18}O$ is -23.27 ± 0.10 and $\delta^{13}C$ is -5.01 ± 0.03 ‰ VPDB. Core GeoB3910-2 *C. wuellerstorfi* $\delta^{13}C$ was measured at the University of Bremen, Germany, on a Finnigan MAT 252 mass spectrometer on samples of 1 to 5 specimens (Heil, 2006), with a mean external reproducibility (1σ) for carbonate standards of ± 0.05 ‰ for $\delta^{13}C$."

p.4-5 (New sedimentary Pa/Th data): How was the discrete sampling performed for Pa/Th? This might be important for direct comparison of Pa/Th to Ti/Ca (from XRFscanning?) during the D-O variability. Are the analyses by both methods exactly performed on the same sediment intervals? Core scanner intervals are often deviating from those that are discretely sampled (e.g., at 1-cm resolution, a measurement at 5 cm is covering the interval from 4.5 to 5.5cm, with an Avaatech core scanner). This might somewhat influence the lead/lag calculations, and may require resampling of the Ti/Ca data (although the impact is probably small).

Pa/Th was measured on discrete 1cm-thick samples, as well as *C. wuellerstorfi* $\delta^{13}C$. In contrast, the use of an Avaatech XRF Core Scanner to measure MD09-3257 elemental ratios allowed us to produce a quasi-continuous MD09-3257 Ti/Ca signal with 1 measurement every

0.5 mm. For the purposes of the present study, we first resampled and dated core MD09-3257 Ti/Ca signal at depth intervals of 0.5 cm. Then, prior to time series analyses, as explained p. 6, lines 7-8, we resampled all three studied time series with constant time steps varying between 50 and 500 y (corresponding to ~0.5 to 5 cm spacing, knowing that the mean sedimentation rate is 10 cm/ky). Therefore, the fact that the initial sample thickness of Pa/Th or *C. wuellerstorfi* $\delta^{13}C$ measurements is different from that of Ti/Ca measurements, has no impact on the lead/lag calculations.

p. 5, lines 19-20: Add shortly why the 232Th is indicative of the vertical terrigenous flux (detrital origin?).

We have modified the sentence

"The ^{230}Th-normalized ^{232}Th flux, hereafter simply referred to as the ^{232}Th flux, is indicative of the vertical terrigenous flux to the core site."

into

"The ^{230}Th-normalized ^{232}Th flux, hereafter simply referred to as the ^{232}Th flux, is indicative of the vertical flux of terrigenous material at the core site, since ^{232}Th is a trace element that is mostly contained in the continental crust (Taylor and McLennan, 1985) and is thus commonly used as a geochemical tracer for material of detrital origin (*e.g.* Anderson et al. (2006))."

p.10, lines 8-12: The uncertainty of the leads and lags in the cross-wavelets should already be given in the Methods (section "cross-correlation and wavelet analysis"). The error propagation is not entirely clear to me, did the authors use a mean squared error (MSE)?

We computed the uncertainty of the leads and lags produced by the wavelet analysis assuming Gaussian error propagation of the two independent uncertainties described p.10, lines 8-12. We computed the total 1σ uncertainty as the square root of the sum of the different variances representing the different sources of uncertainty taken into account. We have clarified this and changed the sentence

"Note that uncertainties for leads and lags given in Table 1 are computed as the propagation of two uncertainties: (i) […] (Fig. 4-6d), and (ii) […] (Fig. 4-6f)."

into

"The uncertainties of the leads and lags (Table 1) are computed assuming Gaussian error propagation of the two following independent uncertainties: (i) […] (Fig. 4-6d), and (ii) […] (Fig. 4-6f)."

However, we cannot move this paragraph from the results section to the methods section because the description of the two independent sources of uncertainty involves the description of the wavelet results given in Figure 4.

p. 11, line 23: Is the cross-correlation really imprecise and unreliable, or does it just lump all frequency signals into one and give you an average output, which is basically correct for the time window that was analyzed? The authors could have used different time windows (e.g., 3000 years and 6000 years) and calculate a running correlation across the whole interval (with one of the records shifted towards the other in different time steps). The result from such a running correlation test will/would be probably very similar to the cross-wavelet analyses. Cross-correlation is not imprecise or unreliable, just not the most suitable method to study non-stationary climate signals. I suggest to change this sentence, and also that at p. 11 line 29, more focusing on the fact that these cross-correlations cannot be used to disentangle the leads/lags of variable frequencies in the proxy records.

Cross-correlation does indeed lump all frequencies. This method thus yields one unique relative phase for the entire studies record, which is meaningless because different portions of the studied records are characterized by different frequencies. Also, as described p. 6 (lines 4-11), cross correlation consists in computing the correlation coefficient between two time series, after having shifted one with respect to the other by increments of the time step (R script given in the supplementary material). The results of this operation are given in Figure 2 and are not similar to the cross-wavelet analyses for the reason given above.

However, we agree that the sentences p. 11, line 23 and line 29 could be improved and that we should insist on the fact that cross-correlation is not a suitable method to study non-stationary climate signals. We have thus modified

"[…] confirms that the latter method yields imprecise and unreliable results when applied to climatic signals"

into

"[…] confirms that the latter method yields imprecise and unreliable results when applied to non-stationary climatic signals",

and

"However, as shown here, cross-correlation does not yield reliable results when applied to climatic signals of the last glacial."

into

"However, as shown here, cross-correlation is not a suitable method to analyze non-stationary climatic signals such as those of the last glacial."

p. 12, line 26: What is the reason to not just use a ln(K/Ca) ratio, instead of ln(Ti/Ca), to circumvent these problems? (Other than the reason that previous studies used Ti/Ca, but probably did not consider these bioturbation effects).

We agree with Referee 1 that it seems judicious to use ln(K/Ca) or ln(Rb/Ca) instead of ln(Ti/Ca) as a proxy of runoff from the adjacent continent. However, the present study builds on previous studies from the same region and cores using ln(Ti/Ca) or Ti/Ca, so we chose to use ln(Ti/Ca) and simply verified if an offset between ln(K/Ca) or ln(Rb/Ca) and ln(Ti/Ca) was detectable.

p.13, line 10: To me it seems that for HS3 there is also not a clear visible lead of Pa/Th relative to ln(Ti/Ca). Is this not what you expect considering that the origin of icebergs/IRD seems to be more European orientated for HS3 (Gwiazda et al., 1996; Henry et al., 2016), while the others find their origin mainly from the Laurentide ice sheet? The reduction in overturning seems to be also much less during HS3 compared to the others.

We agree that the reduction in overturning as recorded by Pa/Th is much smaller during HS3 compared to the other Heinrich stadials. Concerning the lead of Pa/Th relative to ln(Ti/Ca) marking the beginning of HS3, the only notable difference between that transition towards higher Pa/Th values and the transitions corresponding to the other Heinrich stadials, is one single Pa/Th data point (dated at ~31 ka) which was not duplicated and makes the transition a little noisy. We thus prefer not to draw firm conclusions from the presence of this single data point.

p.13, line 20: Doesn't the 232Th flux show that the vertical terrigenous flux was largest during HS4?

We thank Referee 1 for this question that led us to realize that the discussion concerning the different phasing observed for Heinrich Stadial 1 than for the Younger Dryas and the other Heinrich stadials had to be modified.

The large ^{232}Th flux recorded during both HS4 and HS1, together with the similarity in Pa/Th and Ti/Ca amplitudes during these two Heinrich stadials indicate that the different phasing observed for Heinrich Stadial 1 is most likely not due to a difference in terrestrial input.

We have thus replaced this portion of the discussion by the following few sentences:

"Such a different sequence of events seems to indicate that in the case of HS1, the increase in rainfall over tropical South America during HS1 was not a response to a decrease in Atlantic overturning circulation. Instead, a southward shift of the low-latitude atmospheric convection zone (Intertropical Convergence Zone, ITCZ), along with its associated maximum in precipitation, could have occured in response to extended north hemisphere ice sheets and sea ice cover without any change in ocean circulation (Chiang et al., 2003). This atmospheric mechanism would have prevailed at the beginning of HS1 because ice sheets reached their maximum extent around that time."

Similarly, we removed the two sentences on this topic from our conclusions and modified the conclusions last sentence into:

"Finally, the relative lead of Pa/Th over ln(Ti/Ca) is visible for the YD and for all Heinrich stadials, except HS1. In the case of HS1, the southward shift of the ITCZ may have been an atmospheric response to the maximum extent in northern high-latitude ice sheets and sea ice cover (Chiang et al., 2003) around that time, rather than a progressive response to a slowdown of the AMOC, as is the case of the other stadials. These different atmospheric and oceanic scenarios remain to be tested by numerical experiments performed over several thousands of years in glacial conditions, whereby climate models compute water and calcite δ^{18}O, DIC δ^{13}C, and sedimentary Pa/Th."

We are grateful to Referee 1 for noticing that the discussion of this aspect of our data in the submitted version of our manuscript was not convincing. We are glad that the revised version is improved in this regard.

p.14, line 27: Is a 2-4cm downward shift also plausible for differential bioturbation? I suppose there is always bioturbation of both fine and coarse particles.

The sentence p.14, line 25 to 27 does indeed concern differential bioturbation. We have clarified this by replacing "bioturbation" by "differential bioturbation".

Technical Comments:

We thank Referee 1 for all his/her comments and advices, not only on the article content but also on its form.

p.2 line 8-10 (“In the best. . .into calendar ages”): Sentence does not read well. Rephrase/break up sentence.

We have replaced the very long sentence

“In the best cases, when marine cores are radiocarbon dated, past surface reservoir ages do not vary too much through time, and bioturbation biases remain limited (e.g. for high sedimentation rates), dating uncertainties mainly derive from the calibration of radiocarbon ages into calendar ages.”

by 2 sentences:

“When marine cores are radiocarbon dated, uncertainties can arise from bioturbation biases (e.g. Lougheed et al. (2018)) and changes in past surface reservoir ages (Waelbroeck et al., 2001; Thornalley et al., 2011). In the best cases, when changes in past surface reservoir ages and bioturbation biases remain limited, dating uncertainties mainly derive from the calibration of radiocarbon ages into calendar ages.”

p.2 line 26: Add when the core was recovered.

Done

p. 3, line 27: Please write “as defined by Rasmussen et al. (2014)”. This should also be done for the other parts of the text where citations are part of the sentence.

Done

p. 8, line 21: Table S2 considers the opal measurements, which Table needs to be referred to?

We thank Referee 1 for having noted this omission. We have added a table (Table S4 in the new numbering) containing the cross-correlation results to the supplementary material.

Figure 1: I think a larger overview map of South America would have been nice here (e.g., Burckel et al., 2015)

We chose this degree of zoom in order to be able to clearly represent the different catchment areas. The rationale behind this choice is to provide the reader with the information on the surface currents and Brazilian rivers that may impact on the terrigenous input at the core site.

Figure S1: Multiplier for ln(Ti/Ca), is this really necessary? Is it not sufficient to change the range on the y-axis?

We opted for that solution for simplicity. Importantly, the scaling by 0.3 of the ln(Ti/Ca) of both cores has no incidence on this supplementary figure showing the alignment of GeoB3910-2 ln(Ti/Ca) to MD09-3257 ln(Ti/Ca).

Figure S1: The unit for the sedimentation rate is missing partially on the y-axis.

Fixed!

References: Burckel, P., Waelbroeck, C., Gherardi, J.-M., Pichat, S., Arz, H., Lippold, J., Dokken, T., and Thil, F.: Atlantic Ocean circulation changes preceded millennial tropical South America rainfall events during the last glacial, Geophys. Res. Lett., 42, 411-418, 2015.

Grant, K.M., Rohling, E.J., Bar-Matthews, M., Ayalon, A., Medina-Elizalde, M., Ramsey, C.B., Satow, C., Roberts, A.P.: Rapid coupling between ice volume and polar temperature over the past 150,000 years. Nature 491, 744-747, 2012.

Gwiazda, R.H., Hemming, S.R., Broecker, W.S.: Provenance of icebergs during Heinrich event 3 and the contrast to their sources during other Heinrich episodes, Paleo- ceanography, 11(4), 371-378, 1996.

Henry, L., McManus, J. F., Curry, W. B., Roberts, N. L., Piotrowski, A. M., and Keigwin, L. D.: North Atlantic ocean circulation and abrupt climate change during the last glaciation, Science, 353, 470-474, 2016.

Jaeschke, A., Rühlemann, C., Arz, H., Heil, G., and Lohmann, G.: Coupling of millennial-scale changes in sea surface temperature and precipitation off northeastern Brazil with high-latitude climate shifts during the last glacial period, 20 Paleoceanography, 22, PA4206, 2007.

Weltje, G.J., Tjallingii, R.: Calibration of XRF core scanners for quantitative geochemical logging of sediment cores: theory and application. Earth and Planetary Science Letters 274, 423-438, 2008.

Referee #2:

Waelbroeck et al. have measured Ti/Ca and Pa/Th in a core taken on the margin of northern Brazil, which records rainfall on the nearby continental area and the strength of the Atlantic meridional overturning circulation at intermediate depths. Since the two measurements are done on the same core, they are able to determine the phase relationship between the two variables with minimum uncertainty, which gives them new insights into the response of the ITCZ to changes in the AMOC. They use wavelet analysis to determine phase lags at different frequencies and show that ITCZ movement lags changes in AMOC both at the D/O and HE frequency, but more so at the HE frequency. They attribute this difference to a positive feedback between the strength of the AMOC, seawater temperature and iceberg discharge, which they had first proposed in an earlier publication. The authors pay due attention to the possible impact of bioturbation on the phase relationship between Ti/Ca and Pa/Th, which they convincingly rule out, and to multiple caveats in the interpretation of Pa/Th in term of circulation changes. The paper is clearly written and provides important new findings. I recommend publication after considering the relatively minor comments below (note, however, that I am unable to provide knowledgeable comments on the technicalities of wavelet analysis).

While the authors have clearly established the lag between Ti/Ca and Pa/Th, their ultimate goal is to establish the lag in the response of the ITCZ to changes in AMOC. I think the authors should also discuss the extent to which there might be lags between processes and proxies. For instance, would a change in AMOC translate instantaneously into a change in Pa/Th in their core? I think this is unlikely. Pa/Th recorded in sediments is controlled by the ratio between lateral transport by circulation and vertical transport by scavenging of the Th and Pa produced in the water column. Even if seawater were flowing from the north Atlantic to the Brazilian margin through a pipe (i.e. changes in deep water formation would translate into an instantaneous change in lateral velocity in the pipe), there should still be a lag between sediment Pa/Th and changes in AMOC, depending on the response time of dissolved Th and Pa in the water column overlying the coring site. While the response time of Th is decadal, the full expression on circulation changes on Pa may take several centuries. In addition, the "pipe" is of course an unrealistic cartoon of the AMOC. In reality, I would expect an additional lag between lateral velocity at the coring site and changes in deep water formation, but at this point this is just intuitive and it is well beyond me to guess how long or how short this lag would be. Nonetheless, I think the authors could bring this up and indicate that the lag between Ti/Ca and Pa/Th should be taken as a minimum of the lag of the response of the ITCZ to changes in AMOC. There might also be a lag between Ti/Ca and the change in the seasonal latitudinal range of position of the ITCZ depending on the location of the region supplying lithogenics to the coring site. For instance, if the region is farther south from the southernmost zone of precipitation before the change in AMOC, it may take more time for the ITCZ to reach this region.

We thank Roger François for this important remark. We agree that we should explicitly mention the fact that a change in AMOC does not translate instantaneously into a change in Pa/Th.

To do so, we have added the following few sentences to the paragraph starting at line 25 on p. 13 "[…] our results indicate that rainfall increases in the region adjacent to MD09-3257 occurred several hundred years after the increase in sedimentary Pa/Th at our core site.":

"Furthermore, this lead of sedimentary Pa/Th over ln(Ti/Ca) should be taken as a minimum lead of AMOC over ln(Ti/Ca) because a change in AMOC does not translate instantaneously into a change in sedimentary Pa/Th. A delay between a change in AMOC and the resulting change in sedimentary Pa/Th is indeed expected, which depends on the propagation time of the circulation change to the core site and on the response time of dissolved Th and Pa in the water column overlying the core site (i.e. 30-40 for ^{230}Th, 100-200 y for ^{231}Pa (François, 2007)). However, increases or decreases in sedimentary Pa/Th should be measurable before the dissolved Th and Pa have fully adjusted to the new circulation regime, especially at sites with high sedimentation rates as our study site. We thus expect this additional delay to be less than 100 y and much smaller than the computed lead of MD09-3257 sedimentary Pa/Th over ln(Ti/Ca)."

Concerning a possible lag between Ti/Ca and the change in the position of the ITCZ, we have specified in the submitted manuscript that our marine core records can only inform on rainfall changes over the catchment area of the rivers which directly deliver sediment to the study site, that is, over the adjacent continent. Rainfall changes in a region located north of this catchment area may occur before the rainfall changes recorded in our marine cores but we have no means to assess such a delay. We thus prefer not add anything on this subject to text.

While the authors have taken into account how changes in scavenging could obscure the interpretation of Pa/Th in terms of circulation, I think it would also be worth mentioning that interpreting changes in circulation from a single core can also be problematic. While it is correct that higher rate of AMOC should result in a lower sediment Pa/Th when averaged over an entire ocean basin, that may not be correct for any core. Depending on the proximity of the coring location to the site of deep water formation, decreasing the AMOC may actually decrease sediment Pa/Th (e.g. Luo et al., 2010; Fig. 14). I would suggest specifying that we would expect to see an increase in Pa/Th with decreasing rate of AMOC at the coring site of this study because it is sufficiently removed from the site of deep water formation.

Accordingly, I would change the wording on line 4-5 p5: "[*when average over an entire ocean basin*], high (low) flow rates therefore result in high (low) Pa export…"

We are aware that a change in AMOC can produce very different sedimentary Pa/Th signals depending on the location of the cores with respect to that of deep water formation, as demonstrated in Luo et al. (2010).

We have changed the wording on line 4-5 p. 5 as recommended, and modified

"High (low) flow rates therefore result in high (low) Pa export…"

into

"When averaged over an entire ocean basin, high (low) flow rates therefore result in high (low) Pa export…"

Also, we agree that deriving the state of AMOC from a single core location is prone to error. MD09-3257 is however located in an area where the measured Pa/Th vertical profile in core top sediments is consistent with a dominant role of the overturning circulation (Lippold et al., 2011), as explained p. 5, line 11-15 of the submitted manuscript.

Line 26, p7: shorter stadial may have lower increase in Pa/Th because they were too short to allow the full expression of the increase in Pa/Th (limited by the response time of Pa in the water column).

The Dansgaard-Oeschger (D-O) stadials discussed in the present paper have durations of about 1000 y, which is much longer than the response time of dissolved Pa in the water column (100-200 y for ^{231}Pa (François, 2007)). Therefore, the response time of dissolved Pa in the water column cannot be the reason for the lower increase in Pa/Th of D-O stadials with respect to Heinrich stadials. Rather, as explained p. 13, lines 27-31 and p. 14 lines 1-2 of the submitted manuscript, we suggest that a positive feedback involving iceberg discharges is only triggered in the case of Heinrich stadials. In contrast, AMOC slowdowns associated with D-O stadials would not trigger such a positive feedback loop and would hence remain limited.

Line 10, p8: (including Pa/Th values susceptible to be partially impacted by large particles flux [*or boundary scavenging resulting from slower AMOC*])

We have added "or boundary scavenging resulting from slower overturning circulation" to the parentheses p. 8, line 10, as recommended.

Line 24, p12: Why not use Th-normalized Ti instead of Ti/Ca to totally eliminate the effect of changes in carbonate dissolution/production?

This is an interesting suggestion. In our manuscript, we relied on the interpretation of the Ti/Ca signal given in former studies of the same area, but our $^{230}Th_{xs,0}$ measurements do indeed give us the opportunity to directly compute Th-normalized Ti flux in order to eliminate the effect of changes in carbonate dissolution and production on the Ti/Ca signal, if any.

We have computed core MD09-3257 Th-normalized Ti signal and compared it with the Ti/Ca and Ti signals in the following figure.

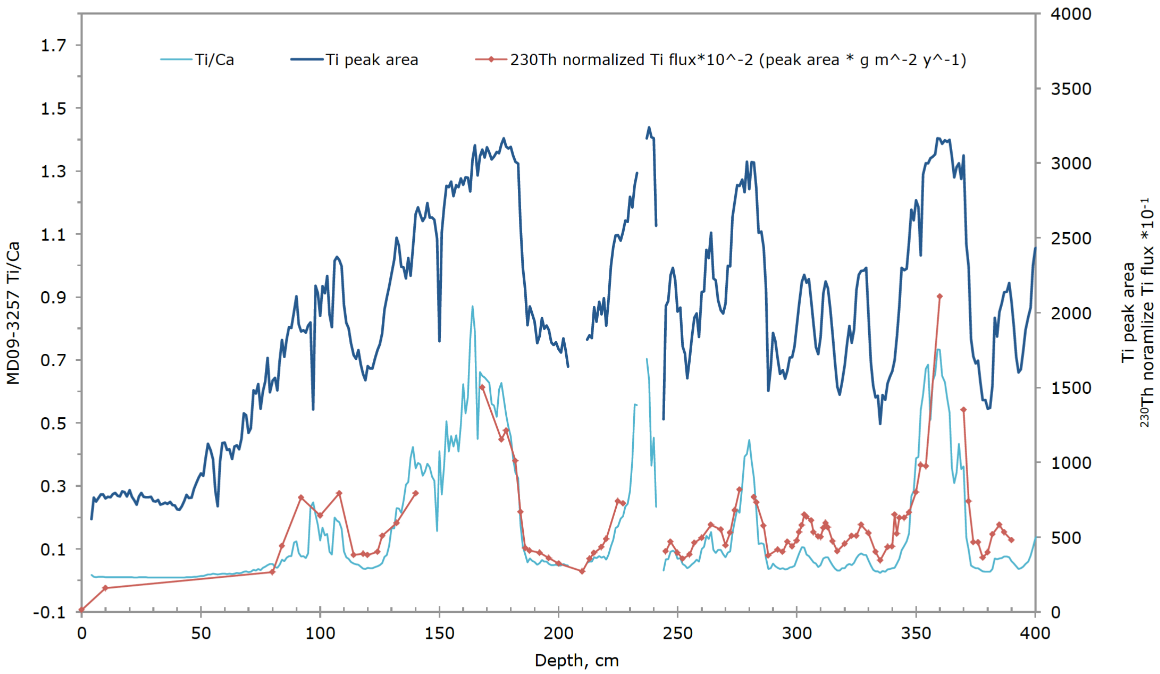

Figure 1. Comparison of core MD09-3257 Th-normalized Ti, Ti/Ca and Ti signals.

We see that the Th-normalized Ti signal is indeed very similar to Ti/Ca, thereby confirming that the Ti/Ca signal is not biased by changes in carbonate dissolution or production.

However, MD09-3257 Th-normalized Ti signal is measured at much lower resolution then MD09-3257 Ti/Ca, and suffers from gaps over the Heinrich stadials. Therefore, the use of MD09-3257 Ti/Ca instead of the Th-normalized Ti signal remains the best option for the present study.

Line 8; p13: Briefly describe what the "independent approach" is.

We have modified the sentence

"This lead is comparable to the relative phase previously estimated between MD09-3257 Pa/Th and Ti/Ca at the onset of HS4 (690 ± 180 y) and HS2 (1420 ± 250 y) respectively, using a completely independent approach (Burckel et al., 2015)."

into

"This lead is comparable to the relative phase previously estimated between MD09-3257 Pa/Th and Ti/Ca at the onset of HS4 (690 ± 180 y) and HS2 (1420 ± 250 y) respectively, based on the identification of the transition in the Pa/Th and Ti/Ca signals at the beginning of these two stadials (Burckel et al., 2015)."

Cited references

Anderson, R., Fleisher, M., and Lao, Y.: Glacial–interglacial variability in the delivery of dust to the central equatorial Pacific Ocean, Earth and Planetary Science Letters, 242, 406-414, 2006.

Bronk Ramsey, C.: Deposition models for chronological records, Quat. Sci. Rev., 27, 42-60, 2008.

Burckel, P., Waelbroeck, C., Gherardi, J.-M., Pichat, S., Arz, H., Lippold, J., Dokken, T., and Thil, F.: Atlantic Ocean circulation changes preceded millennial tropical South America rainfall events during the last glacial, Geophys. Res. Lett., 42, 411-418, 2015.
Chiang, J. C. H., Biasutti, M., and Battisti, D. S.: Sensitivity of the Atlantic Intertropical Convergence Zone to Last Glacial Maximum boundary conditions, Paleoceanography, 18, doi:10.1029/2003PA000916, 2003.
Croudace, I., and Rothwell, R.: Micro-XRF studies of sediment cores, Dev. Paleoenviron. Res., 17, 2015.
François, R.: Chapter Sixteen Paleoflux and Paleocirculation from Sediment 230 Th and 231 Pa/230 Th, Developments in Marine Geology, 1, 681-716, 2007.
Freeman, E., Skinner, L. C., Waelbroeck, C., and Hodell, D.: Radiocarbon evidence for enhanced respired carbon storage in the Atlantic at the Last Glacial Maximum, Nat Commun, 7, 10.1038/ncomms11998, 2016.
Heil, G.: Abrupt climate shifts in the western tropical to subtropical Atlanic region during the last glacial, PhD Thesis, Bremen University, 121 pp., 2006.
Jaeschke, A., Rühlemann, C., Arz, H., Heil, G., and Lohmann, G.: Coupling of millennial-scale changes in sea surface temperature and precipitation off northeastern Brazil with high-latitude climate shifts during the last glacial period, Paleoceanography, 22, PA4206, doi:4210.1029/2006PA001391, 2007.
Key, R. M., Kozyr, A., Sabine, C. L., Lee, K., Wanninkhof, R., Bullister, J. L., Feely, R. A., Millero, F. J., Mordy, C., and Peng, T. H.: A global ocean carbon climatology: Results from Global Data Analysis Project (GLODAP), Global biogeochemical cycles, 18, 2004.
Lippold, J., Gherardi, J.-M., and Luo, Y.: Testing the 231Pa/230Th paleocirculation proxy: A data versus 2D model comparison, Geophys. Res. Lett., 38, doi:10.1029/2011GL049282, 2011.
Lougheed, B. C., Metcalfe, B., Ninnemann, U. S., and Wacker, L.: Moving beyond the age–depth model paradigm in deep-sea palaeoclimate archives: dual radiocarbon and stable isotope analysis on single foraminifera, Climate of the Past, 14, 515-526, 2018.
Luo, Y., Francois, R., and Allen, S. E.: Sediment 231Pa/230Th as a recorder of the rate of the Atlantic meridional overturning circulation: insights from a 2-D model, Ocean Science, 6, 381-400, 2010.
Reimer, P., Bard, E., Bayliss, A., Beck, J. W., Blackwell, P. G., Bronk Ramsey, C., Buck, C. E., Cheng, H., Edwards, R. L., Friedrich, M., Grootes, P. M., Guilderson, T. P., Haflidason, H., and ... IntCal13 and Marine13 radiocarbon age calibration curves 0–50,000 years cal BP, Radiocarbon, 55, 1869–1887, 2013.
Taylor, S., and McLennan, S.: The continental crust: its composition and evolution, Oxford: Blackwell Press, 312 pp., 1985.
Thornalley, D. J. R., Barker, S., Broecker, W. S., Elderfield, H., and McCave, I. N.: The Deglacial Evolution of North Atlantic Deep Convection, Science, 331, 202-205, 2011.
Vazquez Riveiros, N., Waelbroeck, C., Roche, D. M., Moreira, S., Burckel, P., Dewilde, F., Skinner, L., Böhm, E., Arz, H. W., and Dokken, T.: Northern origin of western tropical Atlantic deep waters during Heinrich Stadials, submitted.
Waelbroeck, C., Duplessy, J.-C., Michel, E., Labeyrie, L., Paillard, D., and Duprat, J.: The timing of the last deglaciation in North Atlantic climate records, Nature, 412, 724-727, 2001.
Weltje, G. J., and Tjallingii, R.: Calibration of XRF core scanners for quantitative geochemical logging of sediment cores: theory and application, Earth and Planetary Science Letters, 274, 423-438, 2008.

Relative timing of precipitation and ocean circulation changes in the western equatorial Atlantic over the last 45 ky

Claire Waelbroeck[1], Sylvain Pichat[2,3], Evelyn Böhm[1], Bryan C. Lougheed[1], Davide Faranda[1], Mathieu Vrac[1], Lise Missiaen[1], Natalia Vazquez Riveiros[1,4], Pierre Burckel[5], Jörg Lippold[6], Helge W. Arz[7], Trond Dokken[8], François Thil[1], Arnaud Dapoigny[1]

[1] LSCE/IPSL, Laboratoire CNRS-CEA-UVSQ, 91198 Gif-sur-Yvette, France
[2] Laboratoire de Géologie de Lyon (LGL-TPE), Ecole Normale Supérieure de Lyon, Université de Lyon, CNRS UMR5276, 69007 Lyon, France
[3] Climate Geochemistry Department, Max Planck Institute for Chemistry, Mainz, Germany
[4] Ifremer, Unité de Geosciences Marines, 29280 Plouzané, France
[5] IPGP, Université Sorbonne, 75238 Paris, France
[6] Institute of Earth Sciences, Heidelberg University, Im Neuenheimer Feld 234, 69120 Heidelberg, Germany
[7] Leibniz-Institute for Baltic Sea Research Warnemünde, Seestrasse 15, 18119 Rostock, Germany
[8] Uni Research and Bjreknes Centre for Climate Research, Nygårdsgaten 112, 5008 Bergen, Norway

Correspondence to: Claire Waelbroeck (claire.waelbroeck@lsce.ipsl.fr)

Abstract. Thanks to its optimal location on the North Brazilian margin, core MD09-3257 records both ocean circulation and atmospheric changes. The latter occur locally in the form of increased rainfall on the adjacent continent during the cold intervals recorded in Greenland ice and northern North Atlantic sediment cores (i.e. Greenland stadials). These rainfall events are recorded in MD09-3257 by peaks in ln(Ti/Ca). New sedimentary Pa/Th data indicate that mid-depth western equatorial water mass transport decreased during all the Greenland stadials of the last 40 ky. Using cross-wavelet transforms and spectrogram analysis, we assess the relative phase between the MD09-3257 sedimentary Pa/Th and ln(Ti/Ca) signals. We show that decreased water mass transport between ~1300 and 2300 m depth in the western equatorial Atlantic preceded increased rainfall over the adjacent continent by 120 to 400 y at Dansgaard-Oeschger (D-O) frequencies, and by 280 to 980 y at Heinrich-like frequencies.

We suggest that the large lead of ocean circulation changes with respect to changes in tropical South American precipitation at Heinrich-like frequencies is related to the effect of a positive feedback involving iceberg discharges in the North Atlantic. In contrast, the absence of widespread ice rafted detrital layers in North Atlantic cores during D-O stadials supports the hypothesis that such a feedback was not triggered in the case of D-O stadials, with circulation slowdowns and subsequent changes remaining more limited during D-O stadials than Heinrich stadials.

1 Introduction

Rapid changes in ocean circulation and climate have been observed in marine sediments and polar ice cores over the last glacial and deglacial period (e.g. Johnsen et al. (1992), Vidal et al. (1997)). These observations demonstrate that the ocean's current mode of circulation is not unique but can rapidly switch between dramatically different states, in conjunction with climate changes, and highlight the non-linear character of the climate system.

Documenting the precise timing and sequence of events in proxy records is a prerequisite to understand the processes responsible for rapid climate changes and improve climate models predictive skills. However, the task is complicated by the difficulty to derive precise age models for marine sediment cores. When marine cores are radiocarbon dated, uncertainties can arise from bioturbation biases (e.g. Lougheed et al. (2018)) and changes in past surface reservoir ages (Waelbroeck et al., 2001; Thornalley et al., 2011). In the best cases, when changes in past surface reservoir ages and bioturbation biases remain limited, dating uncertainties mainly derive from the calibration of radiocarbon ages into calendar ages.

In those cases, errors are less than 150 y for the time interval 0-11 calendar ky BP (ky before 1950, noted ka), of about 400 y for the 11-30 ka interval, and of 600 to 1100 y for 30-40 ka (Reimer et al., 2013). Minimum relative dating errors between records from different marine sediment cores, or between marine and ice cores records, thus reach 500 y at the end of the last deglaciation and increase from 500 to 1500 y, for increasing ages between 11 and 40 ka. It is thus not possible to quantify leads or lags of less than 500 y between records from different marine cores, or between marine and ice core records.

Here we take advantage of the fact that the North Brazilian margin core MD09-2357 records both ocean circulation and atmospheric changes. On the one hand, we reconstruct ocean circulation changes based on new sedimentary Pa/Th data and on epifaunal benthic isotopic ratios. On the other hand, sediment Ti/Ca measured by X-ray fluorescence ~~(XRF)~~ reflects past changes in rainfall on the adjacent continent (Arz et al., 1998 ; Jaeschke et al., 2007). Because Pa/Th and Ti/Ca are recorded in the same core, their relative phasing can be examined with virtually no relative dating uncertainty.

We first present the new sedimentary Pa/Th data and their relation to changes in mid-depth water transport in the western equatorial Atlantic over the last 45 ky. We then precisely assess the relative phasing between the changes in rainfall and in ocean circulation recorded in core MD09-3257.

2 Material and methods

Cores location

Core MD09-3257 (04°14.7'S, 36°21.2'W, 2344 m) was recovered in 2009 from the North Brazilian margin during the R/V Marion Dufresne cruise MD173/RETRO3 at approximately the same position as core GeoB3910-2 (04°14.7'S, 36°20.7'W, 2362 m) (Arz et al., 2001; Jaeschke et al., 2007). Improved recovery of deep-sea sediments with no or little deformation of sediment layers was achieved thanks to the systematic use of the CINEMA software (Bourillet et al., 2007; Woerther and Bourillet, 2005). This software computes the amplitude and duration of the aramid cable elastic recoil, as well as the piston displacement throughout the coring phase, accounting for the length of the cable (water depth) and total weight of the coring system.

At present, the North Brazilian margin is bathed by southward flowing upper North Atlantic Deep Water (NADW) at these depths (Lux et al., 2001; Schott et al., 2003; Rhein et al., 2015) (Fig. 1). Southward advection of dense waters formed at higher northern latitudes is channeled through the western boundary current (Rhein et al., 2015), meaning that our sediment cores are ideally located to detect changes in the transport of northern-sourced waters above 2500 m depth.

X-ray fluorescence spectrometry

Elemental composition was measured employing nondestructive, profiling X-ray fluorescence (XRF) spectrometry. The measurements were made using an AVAATECH XRF Core Scanner at the Bjerkness Centre for Climate Research, Bergen (Norway) at intervals of 0.5 mm on core MD09-3257, and using a CORTEX XRF Scanner at the Bremen Integrated Ocean Drilling Program core repository at intervals of 0.4 cm on core GeoB3910-2 (Jaeschke et al., 2007). This automated scanning method allows for a rapid qualitative determination of the geochemical composition of the sediment at very high resolution (Croudace and Rothwell, 2015).

Chronology

Ti/Ca records from core MD09-3257 and GeoB3910-2 exhibit marked peaks corresponding to increased terrigenous input due to enhanced precipitation and runoff from the continent (Arz et al., 1998 ; Jaeschke et al., 2007) (Fig. 2). These precipitation events are also recorded in South American speleothems, and have been shown to correspond to North Atlantic cold stadial periods (Cheng et al., 2013). The core GeoB3910-2 radiocarbon (^{14}C) age model shows that increases in sedimentary Ti/Ca are indeed synchronous with decreases in South American speleothem $\delta^{18}O$ (Burckel et al., 2015). Based on the observed synchronicity, composite age models of core MD09-3257 and GeoB3910-2 have been developed by using ^{14}C dating for the past 35 ky, combined with the alignment of sediment Ti/Ca increases with decreases in speleothem $\delta^{18}O$ for the older portion of the cores (Vazquez Riveiros et al., submitted), thus transferring the speleothem ages beyond 35 ~~calendar ky BP (~~ka~~)~~ to the marine cores. The chronology of core GeoB3910-2 is based on 17 monospecific radiocarbon dates between 0 and 31 ka (Burckel et al., 2015; Jaeschke et al., 2007). The Ti/Ca record of core GeoB3910-2 was aligned to that of core MD09-3257 in order to transfer the radiocarbon dates of GeoB3910-2 over the interval 12–36 ka to this nearby core. In addition, five monospecific radiocarbon dates over 1–21 ka were obtained directly on core MD09-3257. Speleothem tie points were used to derive the chronology of this core over 38–48 ka (Table S1 and S2) (Vazquez Riveiros et al., submitted).

All radiocarbon dates were converted to calendar dates using the OxCal 4.2 software, the IntCal13 calibration curve (Reimer et al., 2013), and a surface water reservoir age of 550 ± 50 y over 0–18 ka (Key et al., 2004), and of 750 ± 250 y over 18–31 ka (Freeman et al., 2016). The final age models of cores GeoB3910-2 and MD09-3257 were obtained using a *P_Sequence* depositional model (Bronk Ramsey, 2008), i.e. a Bayesian algorithm producing posterior probability distributions for each core depth (Table S1 and S2) (Vazquez Riveiros et al., submitted).

In the present study, the GeoB3910-2 age scale for the 32-50 ka interval was further adjusted by precise alignment of GeoB3910-2 XRF to the MD09-3257 XRF signal (Fig. S1), thereby producing a composite record from these two nearby cores. Given that both XRF signals are virtually identical and measured at very high resolution (sampling step ≤ 0.5 cm), the mean relative dating uncertainty between the two cores is extremely small and is less than 105 y (Fig. S1).

Here, we use XRF ln(Ti/Ca) rather than Ti/Ca because log-ratios provide a unique measure of sediment composition, in contrast to simple ratios, which are asymmetric (i.e. conclusions based on evaluation of A/B cannot be directly translated into equivalent statements about B/A) and hence suffer from statistical intractability (Weltje and Tjallingii, 2008). ~~small precipitation events are more clearly marked in ln(Ti/Ca) than in Ti/Ca.~~ We adopt the same terminology as in Burckel et al. (2015) and define the larger ln(Ti/Ca) peaks as precipitation events PE0 to PE5, with PE0 occurring during the Younger Dryas, and PE1 to PE5 occurring during Heinrich stadials 1 to 5 (Fig. 2). What we refer to as Heinrich stadials are strictly those stadials characterized by the occurrence of iceberg discharges in the mid- to high-latitude North Atlantic. We refer to smaller ln(Ti/Ca) peaks corresponding to D-O stadials by using the Greenland stadial numbering system, as defined by Rasmussen et al. (2014).

Benthic isotopes

Epifaunal benthic foraminifers of the *Cibicides wuellerstorfi* species were handpicked in the >150 µm size fraction (Vazquez Riveiros et al., submitted). Core MD09-3257 *C. wuellerstorfi* $^{13}C/^{12}C$ ($\delta^{13}C$, expressed in ‰ versus Vienna Pee-Dee Belemnite, VPDB) was measured at the LSCE on Finnigan Δ+ and Elementar Isoprime mass spectrometers on samples of 1 to 3 specimens. VPDB is defined with respect to the NBS-19 calcite standard ($\delta^{18}O$ = -2.20 ‰ and $\delta^{13}C$ = +1.95 ‰). The mean external reproducibility (1σ) of carbonate standards is ± 0.03 ‰ for $\delta^{13}C$; measured NBS-18 $\delta^{18}O$ is -23.27 ± 0.10 and $\delta^{13}C$ is -5.01 ± 0.03 ‰ VPDB. Core GeoB3910-2 *C. wuellerstorfi* $\delta^{13}C$ was measured at the University of Bremen, Germany, on a Finnigan MAT 252 mass spectrometer on samples of 1 to 5 specimens (Heil, 2006), with a mean external reproducibility (1σ) for carbonate standards of ± 0.05 ‰ for $\delta^{13}C$. A composite high-resolution benthic isotopic record was generated by combining isotopic data from the upper 294 cm of core MD09-3257 (covering the last 32 ky) with isotopic data from the interval 246-451 cm in core GeoB3910-2 for the older part of the record (Vazquez Riveiros et al., submitted).

The $^{13}C/^{12}C$ isotopic ratio ($\delta^{13}C$, expressed in ‰ versus VPDB) of the epifaunal benthic foraminifer *C. wuellerstorfi* has been shown to record the $\delta^{13}C$ of bottom-water dissolved inorganic carbon (DIC) with minor isotopic fractionation (Duplessy et al., 1984; Zahn et al., 1986; Schmittner et al., 2017). A water mass' initial DIC isotopic concentration is governed by surface productivity in its formation region (i.e., the preferential consumption of ^{12}C by primary productivity, thereby increasing dissolved $\delta^{13}C$), as well as temperature dependent air-sea exchanges (Lynch-Stieglitz et al., 1995). DIC $\delta^{13}C$ subsequently decreases as deep water ages, due to progressive remineralization at depth of relatively ^{13}C-depleted biogenic material. As a result, DIC $\delta^{13}C$ largely follows water mass structure and circulation in the modern ocean, and *C. wuellerstorfi* $\delta^{13}C$ ($\delta^{13}C_{Cw}$ hereafter) has been used to trace water masses and as a proxy of bottom water ventilation (Duplessy et al. (1988) and numerous subsequent studies). A recent study further highlighted that DIC $\delta^{13}C$ more faithfully follows water oxygen content than phosphate content (Eide et al., 2017), lending strong support to the use of $\delta^{13}C_{Cw}$ as a proxy for bottom water ventilation, the term ventilation here referring to the transmission of oxygen-rich, atmosphere-equilibrated water to the ocean interior.

New sedimentary Pa/Th data

New sedimentary ($^{231}Pa_{xs,0}/^{230}Th_{xs,0}$) measurements (excess activity ratio at the time of deposition, Pa/Th hereafter) were produced in core MD09-3257 in order to extend the Pa/Th record of Burckel et al. (2015) and to cover the entire time interval 10-43 ka (Table S3). The excess activity corresponds to the fraction of each radioisotope produced in the water column by U decay and is transferred to the sediment by adsorption on particles sinking in the water column. ^{230}Th and ^{231}Pa excess activities are calculated from bulk sediment measurement by correcting for the contribution of the detrital and authigenic fractions (François et al., 2004; Henderson and Anderson, 2003) using a detrital ($^{238}U/^{232}Th$) value of 0.5 ± 0.1 (2σ) (Missiaen et al., in press). These excess activities are then further corrected from radioactive decay since the time of sediment deposition. Bulk sediment measurements were performed by isotopic dilution mass spectrometry on the LSCE MC-ICP-MS (Neptune^{Plus}, Thermo Fischer), following a method derived from Guihou et al. (2010). Error bars (2 standard deviations) on Pa/Th measurements were computed by Monte Carlo runs (Missiaen et al., in press), accounting for the uncertainties in Pa, Th and U measurements, as well as those of the detrital ($^{238}U/^{232}Th$) value, spike calibrations and dating.
Sedimentary Pa/Th can be used to reconstruct changes in the renewal rate of water masses overlying the core site. This tracer has been successfully used to reconstruct past changes in deep Atlantic circulation intensity (Burckel et al. (2015) and references therein). ^{231}Pa and ^{230}Th are produced at a constant Pa/Th activity ratio of 0.093 by dissolved uranium, which is homogeneously distributed in oceans. ^{230}Th is much more particle reactive than ^{231}Pa, as reflected by their respective residence time in the ocean (30-40 y for ^{230}Th, 100-200 y for ^{231}Pa (François, 2007)). ^{230}Th is therefore rapidly removed from the water column to the underlying sediment, while ^{231}Pa can be advected by oceanic currents. When averaged over an entire

ocean basin, high (low) flow rates therefore result in high (low) ^{231}Pa export and hence low (high) sedimentary Pa/Th ratio. In contrast to $\delta^{13}C_{Cw}$, which records the DIC $\delta^{13}C$ of bottom waters at the core site, sedimentary Pa/Th does not reflect the flow rate at the seabed but that of a water layer of a few hundreds to more than 1000 m above the seafloor (Thomas et al., 2006).

Several potential caveats of the proxy were tested. In particular, ^{231}Pa has a higher affinity for opal than for the other types of particles (Chase et al., 2002) so that high opal fluxes can result in high sedimentary Pa/Th values even in the presence of lateral advection. Similarly, areas of very high vertical particle flux, such as the Atlantic off Western Africa, are characterized by high Pa/Th values (Yu et al., 1996; François, 2007; Lippold et al., 2012). Recent studies have shown that the caveats that may apply to this proxy in some areas do not apply to the western tropical Atlantic region. More specifically, a study including core top material from the western tropical Atlantic margin and using a 2-D model (Luo et al., 2010) showed that the measured Pa/Th vertical profile is consistent with a dominant role of the overturning circulation, rather than particle scavenging, thereby demonstrating that Pa/Th can be used to record changes in water mass overturning rates in that region (Lippold et al., 2011). However, because there are large increases in terrigenous material deposition on the north-east Brazilian margin during the last glacial, we carefully evaluated/assessed if increased terrigenous deposition may have impacted Pa/Th values.

The ^{230}Th-normalized ^{232}Th flux, hereafter simply referred to as the ^{232}Th flux, is indicative of the vertical terrigenous flux to the core site, since ^{232}Th is a trace element that is mostly contained in the continental crust (Taylor and McLennan, 1985) and is thus commonly used as a geochemical tracer for material of detrital origin (e.g. Anderson et al. (2006)). Besides the main precipitation events PE0 to PE4, there is no significant correlation between the Pa/Th ratio and the ^{232}Th flux ($r = 0.21$, $p = 0.07$) (Fig. S2 and S3). In contrast, because the correlation between Pa/Th and the ^{232}Th flux becomes significant ($r = 0.57$, $p << 0.001$) when including the main precipitation events (Fig. S3), the high Pa/Th values observed during PE0 to PE4 could be partly caused by increased terrigenous flux and should be interpreted with caution (empty symbols in Fig. 2). Note that a possible terrigenous influence during the main precipitation events does not preclude that the high Pa/Th values during these periods reflect an almost halted oceanic circulation above the core site. Indeed, Pa scavenging by boundary scavenging can be intensified in times of reduced overturning circulation due to boundary scavenging becoming the main control on sedimentary Pa/Th.

Another source of possible biases in Pa/Th results from variations in opal flux (Chase et al., 2002). However, the North Brazilian margin is known for its low siliceous primary production (Arz et al., 1998). This is confirmed by ^{230}Th-normalized opal flux measurements in MD09-3257, which are below 0.06 g cm^{-2} ky^{-1} (Fig. S3). Moreover, outside of precipitation events PE0 to PE4, there is no correlation between Pa/Th and opal flux (Fig. S3). In conclusion, we may consider that outside of the main precipitation events, our Pa/Th record can be interpreted in terms of changes in the strength of overturning circulation above MD09-3257 coring site.

Cross-correlation and wavelet analysis

Assuming that there exists a constant phase shift between two time series over their entire length, one can perform a simple cross-correlation analysis and compute how the correlation coefficient between the two time series varies as a function of the time lag between the two series (e.g. Davis (1986)).

We normalized (i.e. subtracted the mean and divided by the standard deviation) and resampled the time series Pa/Th, $\delta^{13}C_{Cw}$ and ln(Ti/Ca) to a common age scale using scenarios with constant time steps varying between 50 and 500 y. We then used the R function cor.test (R package *stats* version 3.2.2) for correlation between paired series (R script in supplementary material) to compute the Spearman correlation coefficient between all pairs of the three time series, after having shifted one with respect to the other by increments of the time step.

Another approach consists of classical spectral analysis methods that examine the coherence and phase between two time series in frequency space, such as Fourier transforms. Fourier transforms involve decomposing a signal in infinite-length oscillatory functions (such as sine waves). As such, these methods also rely on the assumption that the decomposition of each signal into characteristic frequencies is valid over its entire length, i.e. that the underlying processes are stationary in time.

In contrast, wavelet analysis can be used to decompose a time series into *time-frequency* space, rather than frequency space, that is, to determine both the dominant modes of variability and how these modes vary in time (Torrence and Compo, 1998). To do so, the wavelet transform decomposes the signal into a sum of small wave functions of finite length that are highly localized in time. Wavelet transform can thus describe changes in frequencies along the studied time series and are particularly relevant for dealing with climatic signals, since they are in essence not stationary in time, but in constant evolution in response to external forcing (i.e. insolation changes), and as a result of internal climate variability.

Given two times series X and Y, with wavelet transforms W^X and W^Y, the cross-wavelet spectrum is defined as $W^{XY} = W^X W^{Y*}$, where W^{Y*} is the complex conjugate of W^Y (Torrence and Compo, 1998). Similarly to Fourier coherency, which is used to identify frequency bands in which two time series are related, the wavelet coherency was developed to identify both frequency bands and time intervals over which the two time series are related. The wavelet coherence between two time series is defined as the square of the smoothed cross-wavelet spectrum normalized by the smoothed individual wavelet power spectra (Torrence and Webster, 1999). This definition resembles that of a traditional correlation coefficient, i.e. wavelet coherence ranges between 0 and 1, and may be viewed as a localized correlation coefficient in time-frequency space (Grinsted et al., 2004).

Analogous to Fourier cross-spectral analysis, the phase difference between two time series can also be computed using a cross-wavelet spectrum. The complex argument arg(W^{XY}) can be interpreted as the local relative phase between X and Y in time-frequency space (Grinsted et al., 2004).

In the present study we use the software developed by Grinsted et al. (2004) to compute the cross-wavelet spectrum, coherence and relative phase between our time series that were normalized and resampled as described before. To test for the persistence of regions of high cross-wavelet coherence, we ran all cross-wavelet analyses 1000 times for each dataset pair (i.e. a Monte Carlo approach). For each of the 1000 runs, each time data point was randomly sampled, whereby a Gaussian distribution of each data point's value (based on the measurement uncertainty) is used to weight the random sampling. Mean and standard deviation values for the coherence and phase direction were calculated using the 1000 runs.

3 Results

3.1 Ocean circulation proxy records

The Pa/Th record of core MD09-3257 now covers the entire 10-43 ka time interval, encompassing the Younger Dryas (YD) and the last four Heinrich stadials (Fig. 2). We have increased its temporal resolution over the time interval 31-38 ka comprising Dansgaard-Oeschger (D-O) events 5 to 8, with respect to the rest of the studied period, in order to examine Atlantic circulation dynamics during D-O events.

Pa/Th data exhibit systematic increases in conjunction with stadials, even if Pa/Th data points that are potentially biased towards elevated values by increased terrigenous input (empty symbols) are discarded. Pa/Th data thus indicate that the renewal rate of the water mass overlying the site decreased during stadials. More specifically, transport of the overlying water mass decreased not only during the YD and Heinrich stadials, but also during practically all D-O stadials. Among D-O stadials, the Pa/Th increase is well marked for GS-7, GS-8 and GS-11, but the signal is too noisy to provide a clear picture for GS-6. This noisy Pa/Th signal is very likely due to sediment reworking, given that the $\delta^{13}C_{Cw}$ record is also noisy over this section of the core. Also, it is noteworthy that no precipitation event is recorded in MD09-3257 or GeoB3910-2 during GS-10 (Fig. 2). There is no clear decrease in the well-dated El Condor (Cheng et al., 2013) speleothem $\delta^{18}O$ records associated with GS-10 either, in contrast with the other Greenland stadials (Burckel et al., 2015). It would seem that there was no apparent increase in precipitation during GS-10 over tropical South America, in contrast to all other GS of the past 40 ky. Overall, longer stadials seem to be associated with larger increases in Pa/Th than shorter stadials.

The $\delta^{13}C_{Cw}$ composite record varies in concert with Pa/Th, with high values indicating the presence of well-ventilated waters during the Holocene and interstadials, and low values indicating a marked reduction in water ventilation during stadials at ~2350 m in the western equatorial Atlantic (Vazquez Riveiros et al., submitted).

3.2 Relative timing of Pa/Th, $\delta^{13}C_{Cw}$ and Ti/Ca

Pa/Th, $\delta^{13}C_{Cw}$ and Ti/Ca are recorded in the same core or in two cores from the same location, which could be precisely aligned through high resolution XRF signals. This situation provides ideal conditions to examine the relative phasing of one proxy with respect to another. Pa/Th and Ti/Ca are recorded in the same core, so their relative phasing can consequently be examined with the smallest possible relative dating uncertainty, whereby the only remaining source of uncertainty is bioturbation. The situation is practically the same when examining $\delta^{13}C_{Cw}$ versus Ti/Ca or $\delta^{13}C_{Cw}$ versus Pa/Th. Apart from the unavoidable uncertainty introduced by bioturbation, the relative dating uncertainty between the $\delta^{13}C_{Cw}$ composite record and any MD09-3257 record is null over 0-32 ka, and amounts to 102 y on average over the 32-50 ka time interval (Fig. S1).

In what follows, we assess the relative phasing between Pa/Th, $\delta^{13}C_{Cw}$ and Ti/Ca, using all Pa/Th data points (including Pa/Th values susceptible to be partially impacted by large particle fluxes or boundary scavenging resulting from slower overturning circulation) in order to have sufficient data to examine periodicities ranging from 1000 to 6000 y. In doing so, we assume that changes in particle fluxes may affect the amplitude of the Pa/Th changes, rather than the timing of these changes. In the following text, we show that excluding the Pa/Th values susceptible to be partially impacted by large particle fluxes does not change our conclusions concerning D-O periodicities (i.e. 1000 to 3000 y).

3.2.1 Average relative phases

We first apply the simple stationary cross-correlation approach to examine how the correlation coefficient of Pa/Th versus ln(Ti/Ca), of $\delta^{13}C_{Cw}$ versus ln(Ti/Ca), and of $\delta^{13}C_{Cw}$ versus Pa/Th, varies as a function of the lag between the different time series (Fig. 3). Prior to computing the correlation coefficient, the three time series were resampled with a time step of 100 y and normalized.

Taken at face value, these results indicate that Pa/Th leads ln(Ti/Ca) (or Ti/Ca) by 200 ± 100 y, that there is no significant phase shift between $\delta^{13}C_{Cw}$ and Ti/Ca, and that $\delta^{13}C_{Cw}$ lags Pa/Th by 200 ± 100 y (Table S4). The uncertainty of ± 100 y directly results from the adopted sampling step of 100 y. In addition, in order to assess the robustness of these results, we applied the same approach to the upper half and lower half of the records. In all cases, we obtained $\delta^{13}C_{Cw}$ lags over Pa/Th of 200 y, and Pa/Th leads over ln(Ti/Ca) of 200 or 300 y, while the phase shift between $\delta^{13}C_{Cw}$ and Ti/Ca remained between -100 and +100 y.

Although this simple method has been applied to climatic time series in previous studies (Langehaug et al., 2016; Henry et al., 2016), such results must be interpreted with caution, since the method has been designed for signals that are stationary in time and is, therefore, not suitable for climatic signals.

3.2.2 Wavelet transforms

The non-stationary character of climatic signals over the last 40 to 45 ky is particularly pronounced. Different typical pseudo-periodicities can be identified for Heinrich and D-O stadials. In the case of Heinrich stadials (corresponding to our main precipitation events), the interval 11.7-49 ka comprises 5 pseudo-cycles that are ~6 to 9 ky long (Fig. 2), such that Heinrich stadials over the studied interval are characterized by an average pseudo-periodicity of about 7 ky. Concerning D-O events, the interval located between HS3 and HS4 (32.5-38.1 ka) comprises 3 pseudo-cycles that are ~1.2, 1.5 and 3 ky long (Fig. 2), yielding an average pseudo-periodicity of about 1.8 ky.

We computed the cross-wavelet spectrum, coherence and phase between ln(Ti/Ca) and Pa/Th (Fig. 4), between $\delta^{13}C_{Cw}$ and Pa/Th (Fig. 5), and between $\delta^{13}C_{Cw}$ and ln(Ti/Ca) (Fig. 6), using the software of Grinsted et al. (2004). The 95% confidence level against red noise is shown as a thick contour line. Relative phases are plotted only for coherences higher than 0.5 (< 0.5 is masked as dark blue). Note that the shaded areas in Fig. 4-6 correspond to the region of the wavelet transform graphs where the edge effects due to the finite length of the time series limit the ability to carry out cross-wavelet analysis. These regions are not considered in our interpretations.

To assess the robustness of our results, we repeated the cross-wavelet transform for different interpolation resolutions ranging from 50 to 500 y and could verify that the features corresponding to the 95% confidence level against red noise for a time step of 100 y are still present at roughly the same time and frequency for other time steps (e.g. see Fig. S4 for results obtained for a time step of 400 y).

Moreover, we ran a spectrogram analysis in order to confirm our wavelet results and avoid any over-interpretation (see Fig. S5 and explicative caption). Unlike the wavelet, the spectrogram analysis is based on a finite time Fourier transform that spans different periods. It provides therefore an alternative base to check wavelet-based results. These tests confirmed the wavelet results for periods comprised between 1 and 6 ky. Beyond 6 ky, wavelet results could not be confirmed by spectrograms due to the short duration of the analyzed records. We do thus not discuss periodicities longer than 6 ky in what follows.

With this in mind, the following regions of significant mean coherence and well-defined mean relative phases can be identified in the cross-wavelet graphs between Pa/Th and ln(Ti/Ca) produced by 1000 Monte Carlo runs (Fig. 4, middle panels): a coherence higher than 0.5 is found for periodicities around 2000 y (ranging from ~1000 to 3000 y) over the time interval ~28-40 ka, and for periodicities around 5000 y (~4000 to 6000 y) over ~25-40 ka. Computing the average phases over each of these two regions, we find that Pa/Th leads ln(Ti/Ca) by 259 ± 140 y (1σ) for periodicities of 1000 to 3000 y over 28-40 ka, and by 631 ± 345 y (1σ) for periodicities of 4000 to 6000 y over 15-40 ka (Table 1).

The cross-wavelet graph between $\delta^{13}C_{Cw}$ and Pa/Th displays slightly different regions of high mean coherence (Fig. 5, middle panels). Examining the same frequency bands as for Pa/Th versus ln(Ti/Ca), we find mean coherences higher than

0.5 for periodicities around 2000 y over ~28-40 ka, and for periodicities around 5000 y over ~15-40 ka. Average phases for these regions indicate that $\delta^{13}C_{Cw}$ lags Pa/Th by 279 ± 244 y (1σ) for periodicities of 1000 to 3000 y over 28-40 ka, but that the lag of $\delta^{13}C_{Cw}$ with respect to Pa/Th for periodicities of 4000 to 6000 y over ~15-40 ka is not significant (Table 1).

Finally, the regions characterized by mean coherences higher than 0.5 between $\delta^{13}C_{Cw}$ and ln(Ti/Ca) are similar to those observed in the graph for Pa/Th and ln(Ti/Ca) (Fig. 6, middle panels). However, the average phases between $\delta^{13}C_{Cw}$ and ln(Ti/Ca) over these regions are not significantly different from zero (Fig. 6d and Table 1), indicating that decreases in $\delta^{13}C_{Cw}$ are in phase with increases in ln(Ti/Ca) within uncertainties.

The uncertainties of the leads and lags (Table 1) are computed assuming Gaussian error propagation of the two following independent uncertainties: (i) the standard deviation of the mean relative phases over the given time-frequency region (Fig. 4-6d), and (ii) the median value of the standard deviation computed by 1000 Monte Carlo runs over the same time-frequency region (Fig. 4-6f). In the case of relative phases between Pa/Th or ln(Ti/Ca) and $\delta^{13}C_{Cw}$, we also accounted for the additional error due to the combining of MD09-3257 and GeoB3910-2 $\delta^{13}C_{Cw}$ records.

We also applied the aforementioned cross-wavelet method only to the subset of Pa/Th data points not affected by large particle fluxes. For the periodicities between ~1000 and 4000 y, the results obtained using this subset (Fig. S6) are virtually unchanged with respect to the results obtained using the entire data set, but coherence decreases for longer periodicities. This decrease is expected because the suppressed data points are all located in the main precipitation events, and hence correspond to the YD and Heinrich stadials.

4 Discussion

4.1 Reconstructed ocean circulation changes over the last 45 ky

Oceanographic studies have shown that the southward transport of northern-sourced waters in the equatorial Atlantic mainly takes place between ~1300 and 4000 m depth in a ~ 100 km wide Deep Western Boundary Current (DWBC) (Lux et al., 2001; Rhein et al., 2015). Using hydrographic, geochemical, and direct velocity measurements acquired in 1993 to inverse an ocean circulation model, Lux et al. (2001) estimated that the volumetric flow of upper ~~North Atlantic Deep Water~~ NADW~~)~~ occupying water depths between ~1300 and 2300 m at 4.5° S within the DWBC is 11.2 Sv (1 Sv = 10^6 m^3 s^{-1}). This estimate is in good agreement with the 10.9 Sv estimated by Schott et al. (2003) based on data from 13 shipboard current-profiling sections taken during the World Ocean Circulation Experiment period 1990-2002.

Our data show that outside of the main precipitation events, the total vertical particle flux did not vary much (remaining within 25.1 ± 3.6 g m^{-2} y^{-1}, 1σ) (Fig. S2). The Pa/Th values of these interstadials are similar or slightly higher than that of the

Late Holocene (Fig. 2), suggesting that the transport of the water mass overlying the core MD09-3257 site was also of ~10 Sv during these interstadials.

It is more difficult to translate the observed increases in Pa/Th during stadials into quantified decreases in water mass transport. However, our new data bring additional observational constraints on the Atlantic circulation changes associated with last glacial millennial climate changes. Two recent studies have indicated that decreases in northern-sourced deep water flow took place during each stadial. On the one hand, increases in Pa/Th during each stadial of the last glacial have been observed at a very deep western North Atlantic site located at ~42 °N and 4500 m depth (Henry et al., 2016). On the other hand, reconstructions of water corrosiveness in a South Atlantic core located at ~44°S and 3800 m depth indicate the absence of northern-sourced deep water at that site during stadials, whereas nearly all interstadials of the last 60 ky are characterized by incursions of northern-sourced deep water into the deep South Atlantic (Gottschalk et al., 2015). Together with these independent results, our results indicate that decreases in both the flow rate and extension of northern-sourced deep waters during stadials were not limited to very dense waters circulating at 3800 m or deeper, but also affected water mass transport above 2350 m in the western equatorial Atlantic.

4.2 Relative timing of Pa/Th, $\delta^{13}C_{Cw}$ and Ti/Ca

4.2.1 Stationary cross-correlation versus cross-wavelet results

Cross-wavelet graphs (Fig. 4-6) show that at the site of MD09-3257, significant coherence and well-defined relative phases between $\delta^{13}C_{Cw}$, Pa/Th and Ti/Ca can be identified in only some regions of the time-frequency space. For instance, when examining the relative phase between $\delta^{13}C_{Cw}$ and Pa/Th over the interval 10-43 ka, a meaningful relative phase can be identified only over ~28-40 ka at D-O frequencies (i.e. periodicities of 1000 to 3000 y) (Fig. 5, Table 1). Furthermore, cross-wavelet results indicate that $\delta^{13}C_{Cw}$ lags Pa/Th by 279 ± 244 y at D-O frequencies, and that decreases in $\delta^{13}C_{Cw}$ are in phase with increases in Pa/Th for periodicities of 4000 to 6000 y (i.e. closer to Heinrich periodicities). This is in contrast with the constant 200±100 lag of $\delta^{13}C_{Cw}$ with respect to Pa/Th obtained by cross-correlation between the two same time series (Fig. 3), and confirms that the latter method yields imprecise and unreliable results when applied to non-stationary climatic signals.

Cross-correlation has nevertheless been recently applied to climatic signals (Langehaug et al., 2016), including Pa/Th and $\delta^{13}C_{Cw}$ records from the last glacial (Henry et al., 2016). In the latter study, cross-correlation between marine records from two deep Bermuda Rise cores and the NGRIP ice oxygen isotopic record was used to infer that deep Bermuda Rise $\delta^{13}C_{Cw}$ led NGRIP by approximately two centuries and that Pa/Th was approximately in phase with NGRIP over the interval 25-60 ka (Henry et al., 2016). The authors further inferred that Pa/Th lags $\delta^{13}C_{Cw}$ by two centuries at their deep Bermuda Rise site. However, as shown here, cross-correlation is not a suitable method to analyze non-stationary climatic signals such as those of the last glacial. Moreover, the inferred relative phases between the marine and NGRIP records are much smaller than the dating error for each individual time series, and, therefore, also the relative dating error of one time series with respect to the other. In summary, the application of stationary cross-correlation techniques and incomplete consideration of geochronological uncertainty casts doubt on the conclusions of the aforementioned studies.

4.2.2 Lead of Pa/Th with respect to ln(Ti/Ca)

Our cross-wavelet results show that MD09-3257 Pa/Th leads ln(Ti/Ca) by 259 ± 140 y (1σ) for periods of 1000 to 3000 y during the ~28-40 ka time interval, and by 631 ± 345 y (1σ) for periods of 4000 to 6000 y during ~15-40 ka (Table 1). Periods of 1000 to 3000 y correspond to pseudo periodicities typical of D-O stadials, while periods of 4000 to 6000 y are close to those of Heinrich stadials. It can be noted that the cross-wavelet results for D-O periodicities are significant only for the ~28-40 ka time interval, which indeed corresponds to the interval of our records for which D-O events are best recorded.
It is important to examine if the observed relative phases could be an artifact due to bioturbation. It has been shown that smaller particles are more likely to be transported by bioturbation than larger particles (Wheatcroft, 1992; McCave, 1988; DeMaster and Cochran, 1982) and that this results in fine particles having apparent younger ages than coarse particles from the same depth in a core (Brown et al., 2001; Sepulcre et al., 2017).
Sedimentary Pa/Th is measured on bulk sediment samples, with dissolved Pa and Th being more readily adsorbed on small particles because of their higher surface to volume ratio (Chase et al., 2002). It has been shown that 50-90% of ^{230}Th excess inventory is found in particles smaller than 10 μm (Kretschmer et al., 2010; Scholten et al., 1994 ; Thomson et al., 1993). It is therefore reasonable to assume that the Pa/Th signal is mostly carried by small particles (< 100 μm).
Assessing the size fraction corresponding to the Ti/Ca signal is more complicated. XRF measurements show that the marked changes in ln(Ti/Ca) recorded in MD09-3257 result from sharp changes in both Ca and Ti concentration in the sediment. Ca is a component of marine calcite and aragonite, and is thus mainly carried by large size fractions of the sediment (> 60 μm). However, previous studies have shown that changes in marine carbonate production and dissolution between 2000 and 3000 m in the western tropical Atlantic were relatively small over the last glacial (Rühlemann et al., 1996 ; Gerhardt et al., 2000). Therefore, the sharp decreases in Ca concentration during stadials result from dilution of marine carbonates by increased input of terrigenous material and the ln(Ti/Ca) signal is driven by changes in terrigenous input, rather than by changes in marine carbonate production or dissolution. It is difficult to assess in which particle size fraction Ti is mostly concentrated. Knowing that Rb and K are typical constituents of clays and, therefore, characteristic of small grain sizes, we verified if a phase shift could be detected between the XRF Ti signal on the one hand, and the XRF Rb and K signals on the other hand. We found no relative offset between Ti and Rb and almost no relative offset between Ti and K, with the inflexion point in the K signal taking place 0.05 cm deeper than in the Ti signal. Given that core MD09-3257 sedimentation rates range from 6

to 14 cm/ky, 0.05 cm corresponds to 5 to 10 y and is thus completely negligible with respect to the observed phase shifts between ln(Ti/Ca) and Pa/Th. We may thus consider that ln(Ti/Ca) and Pa/Th are both carried by small particles and that the observed phase shifts between these two signals are not the result of bioturbation.

Finally, if, against all likelihood, bioturbation were responsible for a lead of Pa/Th with respect to ln(Ti/Ca), such a lead would be independent from the examined periodicity. We may, therefore, reasonably assume that the observed lead of Pa/Th with respect to ln (Ti/Ca) is not an artifact resulting from bioturbation.

We compute a 631 ± 345 y (1σ) lead for Pa/Th over ln(Ti/Ca) by cross-wavelet analysis for frequencies close to those characterizing Heinrich stadials. This lead is comparable to the relative phase previously estimated between MD09-3257 Pa/Th and Ti/Ca at the onset of HS4 (690 ± 180 y) and HS2 (1420 ± 250 y) respectively, based on the identification of the transition in the Pa/Th and Ti/Ca signals at the beginning of these two stadials (Burckel et al., 2015). The large lead of Pa/Th with respect to ln(Ti/Ca) is indeed clearly visible for the YD and all Heinrich stadials, except HS1 (Fig. 2). The apparent synchronicity of the Pa/Th and ln(Ti/Ca) signals at the onset of HS1 in core MD09-3257, as also recently observed in another core of the northern Brazilian margin (Mulitza et al., 2017), suggests that the sequence of events was different at the beginning of HS1 from the one at the beginning of the YD and other Heinrich stadials. Such a different sequence of events seems to indicate that in the case of HS1, the increase in rainfall over tropical South America during HS1 was not a response to a decrease in Atlantic overturning circulation. Instead, a southward shift of the low-latitude atmospheric convection zone (Intertropical Convergence Zone, ITCZ), along with its associated maximum in precipitation, could have occured in response to extended north hemisphere ice sheets and sea ice cover without any change in ocean circulation (Chiang et al., 2003). This atmospheric mechanism would have prevailed at the beginning of HS1 because ice sheets reached their maximum extent around that time. ~~Also of note are the anomalously high sedimentary Pa/Th values at the onset of HS1, which are likely related to extremely high terrigenous particle fluxes (Fig. S2). Records of organic matter proxies from core GeoB3910-2 and a neighboring North Brazilian core show that Heinrich stadials were characterized by a specific sequence of events, whereby increased rainfall firstly led to an initial outwash of organic matter-depleted mineral matter (e.g. exposed shelf sediments or eroded topsoil), after which vegetation cover subsequently developed and reduced erosional processes (Dupont et al., 2010; Jennerjahn et al., 2004). We suggest that lower sea levels during the last glacial maximum caused larger area of shelf to be exposed to erosion, resulting in a larger initial outwash for PE1 than for the other main precipitation events. As a consequence, it seems likely that exceptionnally large vertical particle fluxes temporarily overprinted the impact of water mass transport changes on MD09-3257 sedimentary Pa/Th ratio at the onset of PE1.~~

Our results ~~further~~ also indicate that a significant lead of Pa/Th with respect to ln(Ti/Ca) is ~~also~~ present at D-O frequencies. Moreover, the lead of Pa/Th with respect to ln(Ti/Ca) is markedly shorter at D-O frequencies (259 ± 140 y) than at Heinrich frequencies (631 ± 345 y).

Climate models ~~do indeed~~ simulate a southward shift of the ~~low latitudes atmospheric convection zone (Intertropical Convergence Zone,~~ ITCZ~~) and associated maximum in precipitation~~ in response to a slowdown of the Atlantic meridional overturning circulation (AMOC), but after only a few years (Dong and Sutton, 2002) ~~see (Kageyama et al., 2010) for a review)~~. In contrast, our results indicate that rainfall increases in the region adjacent to MD09-3257 occurred several hundred years after the increase in sedimentary Pa/Th at our core site. Furthermore, this lead of sedimentary Pa/Th over ln(Ti/Ca) should be taken as a minimum lead of AMOC over ln(Ti/Ca) because a change in AMOC does not translate instantaneously into a change in sedimentary Pa/Th. A delay between a change in AMOC and the resulting change in sedimentary Pa/Th is indeed expected, which depends on the propagation time of the circulation change to the core site and on the response time of dissolved Th and Pa in the water column overlying the core site (i.e. 30-40 for ^{230}Th, 100-200 y for ^{231}Pa (François, 2007)). However, increases or decreases in sedimentary Pa/Th should be measurable before the dissolved Th and Pa have fully adjusted to the new circulation regime, especially at sites with high sedimentation rates as our study site. We thus expect this additional delay to be less than 100 y and much smaller than the computed lead of MD09-3257 sedimentary Pa/Th over ln(Ti/Ca).

A mechanism has been proposed by Burckel et al. (2015) to explain the large lead of AMOC slowdowns during Heinrich and D-O stadials with respect to precipitation events over tropical South America. In this scenario, AMOC slowdowns are progressively amplified through a positive feedback linking the decrease in deep water formation to subsurface warming at high northern latitudes (Mignot et al., 2007; Alvarez-Solas et al., 2013), leading in the case of Heinrich stadials, to erosion of ice shelves and iceberg discharges, which in turn reinforce the initial AMOC slowdown. In contrast, AMOC slowdowns associated with D-O stadials would not trigger such a positive feedback loop and would hence remain limited.

Alternatively, or in addition to an actual lead of the changes in AMOC with respect to precipitation events over tropical South America, another factor could induce a lead of Pa/Th with respect to ln(Ti/Ca) in core MD09-3257. It has been shown that the North Brazil Current (NBC) is able to transport terrigenous material laterally (Allison et al., 2000). Also, different studies have shown that a weakening of the AMOC is associated with a decrease of the NBC transport, taking place not only on decadal timescales (Zhang et al., 2011), but also during the YD and HS1 (Arz et al., 1999; Wilson et al., 2011). Based on this evidence, a recent study suggested that a reduced NBC during HS1 allowed the enhanced input of terrigenous material to settle down on the continental margin offshore North-East Brazil, instead of being transported northward (Zhang et al., 2015). It thus seems possible that terrestrial input would be deviated northward as long as the NBC is vigorous and reach the core site only once the NBC and AMOC are sufficiently reduced, thereby yielding a time-delayed peak in ln(Ti/Ca). If this is the case, the lag of the terrestrial input signal with respect to the Pa/Th signal would be partially or totally caused by the impact of the NBC on terrigenous material deposition (Zhang et al., 2015). The exceptionnal synchronicity of the onset of terrigenous influx and AMOC slowdown at the beginning of HS1 could, therefore, be due to the exceptionnally large fluxes of large grain size material eroded from the proximal exposed shelf during low eustatic sea level, which would have rained down through the water column, even before full reduction of the NBC.

However, in the absence of direct measurements of the NBC velocity and vertical particle flux on the North-East Brazilian margin, the actual delay of terrestrial input with respect to NBC slowdown remains speculative.

4.2.3 Lag of $\delta^{13}C_{Cw}$ with respect to Pa/Th

Our cross-wavelet results show that at MD09-3257 site, $\delta^{13}C_{Cw}$ lags Pa/Th by 279 ± 244 y (1σ) at D-O frequencies over ~28-40 ka (Table 1).

$\delta^{13}C_{Cw}$ is measured using > 150 µm foraminifers ~~(Vazquez Riveiros et al., submitted)~~ and is thus carried by much larger particles than the Pa/Th signal. In that case, differential bioturbation mixing processes would lead to Pa/Th being carried by sediment material younger than the epibenthic foraminifers sampled within the same depth interval. Bioturbation may thus induce an artificial lead of Pa/Th with respect to $\delta^{13}C_{Cw}$. Knowing that the sedimentation rate of MD09-3257 and GeoB3910-2 varies between 6 and 14 cm over the interval 28-40 ka, a 280 y lead translates into a downward shift of 2 to 4 cm in the sediment column, which seems a plausible effect of differential bioturbation.

In conclusion, the lag of $\delta^{13}C_{Cw}$ with respect to Pa/Th at D-O frequencies during ~28-40 ka is likely an artifact resulting from the differential bioturbation of fine and coarse particles. The same differential bioturbation processes likely also affect the relative phase between $\delta^{13}C_{Cw}$ and ln (Ti/Ca). We will thus not further discuss the results of the cross-wavelet analyses involving $\delta^{13}C_{Cw}$.

5 Conclusions

New sedimentary Pa/Th data from core MD09-3257 located on the North Brazilian margin (~4°S, 36°W) at ~2350 m depth indicate decreases in water mass transport above the core site during all Greenland stadials of the last 45 ky. Together with two other recent studies (Gottschalk et al., 2015 ; Henry et al., 2016), these results demonstrate that all stadials of the last 45 ky were not only characterized by decreases in flow rate and extension of northern-sourced waters below 3800 m depth, but also by decreases in mid-depth water mass transport in the western equatorial Atlantic.

Due to its exceptional location, core MD09-3257 records both ocean circulation and atmospheric changes. Ocean circulation changes induce changes in sedimentary Pa/Th and $\delta^{13}C_{Cw}$, whereas changes in precipitation over the adjacent continent induce changes in marine sediments Ti/Ca.

Using cross-wavelet transforms and spectrogram analysis, we were able to precisely and robustly assess the relative phase between MD09-3257 sedimentary Pa/Th and ln(Ti/Ca) signals over the interval 10-43 ka with minimal uncertainty, thanks to both signals being recorded in the same sediment core. We show that Pa/Th leads ln(Ti/Ca) by 259 ± 140 y (1σ) at D-O frequencies over 28-40 ka, and by 631 ± 345 y (1σ) for periodicities close to Heinrich periodicities (4000 to 6000 y) over 15-40 ka.

~~The relative lead of Pa/Th over ln(Ti/Ca) is indeed clearly visible for the YD and all Heinrich stadials, except HS1. We suggest that the apparent synchronicity of the Pa/Th and ln(Ti/Ca) signals at the onset of HS1 in core MD09-3257 may be explained by low eustatic sea level and exceptionnally large fluxes of material eroded from the proximal exposed shelf, which may have temporarily overprinted the impact of water mass transport changes on the sedimentary Pa/Th ratio~~.

In other words, our cross-wavelet transforms and spectrogram analysis results show that changes in water mass transport between ~1300 and 2300 m depth in the western equatorial Atlantic (i.e. within a ~1000 m water layer above MD09-3257 core site) preceded changes in precipitation over the adjacent continent by 110 to 400 y at D-O frequencies, and by 280 to 980 y at Heinrich-like frequencies.

We suggest that the large lead of ocean circulation changes with respect to tropical South American precipitation changes at Heinrich-like ~~frequencies~~ and D-O frequencies is likely related to the action of a positive feedback in the case of Heinrich stadials, in agreement with Burckel et al. (2015). In that case, an AMOC slowdown would lead to sub-surface warming at high northern latitudes, inducing ice-sheet calving and iceberg discharges that would in turn reinforce the initial AMOC slowdown. In contrast, the absence of marked ice rafted detritus layers in North Atlantic sediments during D-O stadials suggests that in the case of D-O stadials, AMOC slowdowns did not trigger such a positive feedback and hence remained limited (Burckel et al., 2015).

Finally, the relative lead of Pa/Th over ln(Ti/Ca) is visible for the YD and for all Heinrich stadials, except HS1. In the case of HS1, the southward shift of the ITCZ may have been an atmospheric response to the maximum extent in northern high-latitude ice sheets and sea ice cover (Chiang et al., 2003) around that time, rather than a progressive response to a slowdown of the AMOC, as is the case of the other stadials. These different atmospheric and oceanic scenarios remain ~~Such a scenario remains~~ to be tested by numerical experiments performed over several thousands of years in glacial conditions, whereby ~~with~~ climate models compute water and calcite $\delta^{18}O$, DIC $\delta^{13}C$, and sedimentary Pa/Th.

Data availability. Data related to this article are available as a supplement file and on Pangaea.

Author contribution. CW and SP designed the research; EB, PB, JL, FT, AD performed the sedimentary Pa/Th measurements; BL performed wavelet analyses; DF and LV contributed expert advices on statistical results and performed spectrogram analyses; LM produced sedimentary Pa/Th values and error bars from MC-ICPMS output; NVR improved the age models of the two cores. CW, NVR and TD participated in the 2009 RETRO coring cruise. HA contributed expert knowledge on the Brazilian margin. CW and TD obtained funding. CW and BL wrote the manuscript.

Competing interests. The authors declare that they have no conflict of interests.

Acknowledgements. This is a contribution to the ACCLIMATE ERC project; the research leading to these results has received funding from the European Research Council under the European Union's Seventh Framework Programme (FP7/2007-2013)/ERC grant agreement n° 339108. Core MD09-3257 was collected on board R/V Marion Dufresne during the 2009 RETRO coring cruise, supported by IPEV, ANR project ANR-09-BLAN-0347 and the ESF EUROMARC project "RETRO". We thank the IPEV team, crew members of R/V Marion Dufresne and all scientists who participated in the 2009 RETRO cruise. We also thank M. Roy-Barman for advices on Pa/Th measurements on LSCE MC-ICP-MS. We acknowledge V. Scao and J. Strømsøe for XRF measurements, C. Moreau, J.-P. Dumoulin, and the UMS ARTEMIS for AMS ^{14}C dates, as well as G. Isguder, L. Mauclair and F. Dewilde for invaluable technical assistance. This is LSCE contribution 6408.

References

Allison, M. A., Lee, M. T., Ogston, A. S., and Aller, R. C.: Origin of Amazon mudbanks along the northeastern coast of South America, Marine Geology, 163, 241-256, 2000.

Alvarez-Solas, J., Robinson, A., Montoya, M., and Ritz, C.: Iceberg discharges of the last glacial period driven by oceanic circulation changes, Proc. Natl. Acad. Sci. USA, doi/10.1073/pnas.1306622110, 2013.

Anderson, R., Fleisher, M., and Lao, Y.: Glacial–interglacial variability in the delivery of dust to the central equatorial Pacific Ocean, Earth and Planetary Science Letters, 242, 406-414, 2006.

Arz, H. W., Pätzold, J., and Wefer, G.: Correlated Millennial-Scale Changes in Surface Hydrography and Terrigenous Sediment Yield Inferred from Last-Glacial Marine Deposits off Northeastern Brazil, Quaternary Research, 50, 157-166, 1998.

Arz, H. W., Pätzold, J., and Wefer, G.: The deglacial history of the western tropical Atlantic as inferred from high resolution stable isotope records off northeastern Brazil, Earth and Planetary Science Letters, 167, 105-117, 1999.

Arz, H. W., Gerhardt, S., Pätzold, J., and Röhl, U.: Millennial-scale changes of surface- and deep-water flow in the western tropical Atlantic linked to Northern Hemisphere high-latitude climate during the Holocene, Geology, 29, 239-242, 2001.

Bronk Ramsey, C.: Deposition models for chronological records, Quat. Sci. Rev., 27, 42-60, 2008.

Brown, L., Cook, G. T., MacKenzie, A. B., and Thomson, J.: Radiocarbon age profiles and size dependency of mixing in northeast Atlantic sediments, Radiocarbon, 43, 929-937, 2001.

Burckel, P., Waelbroeck, C., Gherardi, J.-M., Pichat, S., Arz, H., Lippold, J., Dokken, T., and Thil, F.: Atlantic Ocean circulation changes preceded millennial tropical South America rainfall events during the last glacial, Geophys. Res. Lett., 42, 411-418, 2015.

Chase, Z., Anderson, R. F., Fleisher, M. Q., and Kubik, P. W.: The influence of particle composition and particle flux on scavenging of Th, Pa and Be in the ocean, Earth and Planetary Science Letters, 204, 215-229, 2002.

Cheng, H., Sinha, A., Cruz, F. W., Wang, X., Edwards, R. L., d'Horta, F. M., Ribas, C. C., Vuille, M., Stott, L. D., and Auler, A. S.: Climate change patterns in Amazonia and biodiversity, Nature communications, 4, ncomms2415, 2013.

Chiang, J. C. H., Biasutti, M., and Battisti, D. S.: Sensitivity of the Atlantic Intertropical Convergence Zone to Last Glacial Maximum boundary conditions, Paleoceanography, 18, doi:10.1029/2003PA000916, 2003.

Croudace, I., and Rothwell, R.: Micro-XRF studies of sediment cores, Dev. Paleoenviron. Res., 17, 2015.

Davis, J. C.: Statistics and data analysis in geology, J. Wiley, New York, 646 pp, 1986.

DeMaster, D. J., and Cochran, J. K.: Particle mixing rates in deep-sea sediments determined from excess 210Pb and 32Si profiles, Earth and Planetary Science Letters, 61, 257-271, 1982.

Dong, B. W., and Sutton, R.: Adjustment of the coupled ocean–atmosphere system to a sudden change in the thermohaline circulation, Geophysical Research Letters, 29, 2002.

Duplessy, J.-C., Shackleton, N. J., Matthews, R. K., Prell, W., Ruddiman, W. F., Caralp, M., and Hendy, C. H.: 13C record of benthic foraminifera in the last interglacial ocean : implications for the carbon cycle and the global deep water circulation, Quaternary Research, 21, 225-243, 1984.

Duplessy, J.-C., Shackleton, N. J., Fairbanks, R. G., Labeyrie, L., Oppo, D., and Kallel, N.: Deepwater source variations during the last climatic cycle and their impact on the global deepwater circulation, Paleoceanography, 3, 343-360, 1988.

~~Dupont, L. M., Schlütz, F., Ewah, C. T., Jennerjahn, T. C., Paul, A., and Behling, H.: Two-step vegetation response to enhanced precipitation in Northeast Brazil during Heinrich event 1, Global Change Biology, 16, 1647-1660, 2010.~~

Eide, M., Olsen, A., Ninnemann, U. S., and Johannessen, T.: A global ocean climatology of preindustrial and modern ocean δ13C, Global Biogeochemical Cycles, 31, 515-534, 2017.

François, R., Frank, M., Rutgers van der Loeff, M. M., and Bacon, M. P.: 230Th normalization: An essential tool for interpreting sedimentary fluxes during the late Quaternary, Paleoceanography, 19, 2004.

François, R.: Chapter Sixteen Paleoflux and Paleocirculation from Sediment 230 Th and 231 Pa/230 Th, Developments in Marine Geology, 1, 681-716, 2007.

Freeman, E., Skinner, L. C., Waelbroeck, C., and Hodell, D.: Radiocarbon evidence for enhanced respired carbon storage in the Atlantic at the Last Glacial Maximum, Nat Commun, 7, 10.1038/ncomms11998, 2016.

Gerhardt, S., Groth, H., Rühlemann, C., and Henrich, R.: Aragonite preservation in late Quaternary sediment cores on the Brazilian Continental Slope: implications for intermediate water circulation, International Journal of Earth Sciences, 88, 607-618, 2000.

Gottschalk, J., Skinner, L. C., Misra, S., Waelbroeck, C., Menviel, L., and Timmermann, A.: Abrupt changes in the southern extent of North Atlantic Deep Water during Dansgaard–Oeschger events, Nature Geoscience, 950-954, doi:10.1038/ngeo2558, 2015.

Grinsted, A., Moore, J. C., and Jevrejeva, S.: Application of the cross wavelet transform and wavelet coherence to geophysical time series, Nonlinear processes in geophysics, 11, 561-566, 2004.

Guihou, A., Pichat, S., Nave, S., Govin, A., Labeyrie, L., Michel, E., and Waelbroeck, C.: Late slowdown of the Atlantic Meridional Overturning Circulation during the Last Glacial Inception: new constraints from sedimentary (231Pa/2303 Th), Earth and Planetary Science Letters, 289, 520-529, 2010.

Heil, G.: Abrupt climate shifts in the western tropical to subtropical Atlanic region during the last glacial, PhD Thesis, Bremen University, 121 pp., 2006.

Henderson, G. M., and Anderson, R. F.: The U-series toolbox for paleoceanography, Reviews in Mineralogy and Geochemistry, 52, 493-531, 2003.

Henry, L., McManus, J. F., Curry, W. B., Roberts, N. L., Piotrowski, A. M., and Keigwin, L. D.: North Atlantic ocean circulation and abrupt climate change during the last glaciation, Science, 353, 470-474, 2016.

Jaeschke, A., Rühlemann, C., Arz, H., Heil, G., and Lohmann, G.: Coupling of millennial-scale changes in sea surface temperature and precipitation off northeastern Brazil with high-latitude climate shifts during the last glacial period, Paleoceanography, 22, PA4206, doi:4210.1029/2006PA001391, 2007.

~~Jennerjahn, T. C., Ittekkot, V., Arz, H. W., Behling, H., Pätzold, J., and Wefer, G.: Asynchronous terrestrial and marine signals of climate change during Heinrich events, Science, 306, 2236-2239, 2004.~~

Johnsen, S., Clausen, H. B., Dansgaard, W., Fuhrer, K., Gundestrup, N., Hammer, C. U., Iversen, P., Jouzel, J., and Stauffer, B.: Irregular glacial interstadials recorded in a new Greenland ice core, Nature, 359, 311, 1992.
~~Kageyama, M., Paul, A., Roche, D., and Van Meerbeeck, C. J.: Modelling glacial climatic millennial-scale variability related to changes in the Atlantic meridional overturning circulation: a review, Quat. Sci. Rev., 29, 2931-2956, 2010.~~
Key, R. M., Kozyr, A., Sabine, C. L., Lee, K., Wanninkhof, R., Bullister, J. L., Feely, R. A., Millero, F. J., Mordy, C., and Peng, T. H.: A global ocean carbon climatology: Results from Global Data Analysis Project (GLODAP), Global biogeochemical cycles, 18, 2004.
Kindler, P., Guillevic, M., Baumgartner, M., Schwander, J., Landais, A., and Leuenberger, M.: Temperature reconstruction from 10 to 120 kyr b2k from the NGRIP ice core, Climate of the Past, 10, 1-16, 2014.
Kretschmer, S., Geibert, W., van der Loeff, M. M. R., and Mollenhauer, G.: Grain size effects on 230 Th xs inventories in opal-rich and carbonate-rich marine sediments, Earth and Planetary Science Letters, 294, 131-142, 2010.
Langehaug, H., Mjell, T., Otterå, O., Eldevik, T., Ninnemann, U., and Kleiven, H.: On the reconstruction of ocean circulation and climate based on the "Gardar Drift", Paleoceanography, 31, 399-415, 2016.
Lippold, J., Gherardi, J.-M., and Luo, Y.: Testing the 231Pa/230Th paleocirculation proxy: A data versus 2D model comparison, Geophys. Res. Lett., 38, doi:10.1029/2011GL049282, 2011.
Lippold, J., Mulitza, S., Mollenhauer, G., Weyer, S., Heslop, D., and Christl, M.: Boundary scavenging at the East Atlantic margin does not negate use of 231Pa/230Th to trace Atlantic overturning, Earth and planetary science letters, 333, 317-331, 2012.
Lougheed, B. C., Metcalfe, B., Ninnemann, U. S., and Wacker, L.: Moving beyond the age–depth model paradigm in deep-sea palaeoclimate archives: dual radiocarbon and stable isotope analysis on single foraminifera, Climate of the Past, 14, 515-526, 2018.
Luo, Y., François, R., and Allen, S. E.: Sediment 231Pa/230Th as a recorder of the rate of the Atlantic meridional overturning circulation: insights from a 2-D model, Ocean Science, 6, 381-400, 2010.
Lux, M., Mercier, H., and Arhan, M.: Interhemispheric exchanges of mass and heat in the Atlantic Ocean in January–March 1993, Deep Sea Research Part I: Oceanographic Research Papers, 48, 605-638, 2001.
Lynch-Stieglitz, J., Stocker, T., Broecker, W. S., and Fairbanks, R. G.: The influence of air-sea exchange on the isotopic composition of oceanic carbon: Observations and modeling, Global Biogeochemical Cycles, 9, 653-665, 1995.
McCave, I.: Biological pumping upwards of the coarse fraction of deep-sea sediments, Journal of Sedimentary Research, 58, 1988.
Mignot, J., Ganopolski, A., and Levermann, A.: Atlantic subsurface temperatures: Response to a shutdown of the overturning circulation and consequences for its recovery, Journal of Climate, 20, 4884-4898, 2007.
Milliman, J. D., Summerhayes, C. P., and Barretto, H. T.: Quaternary sedimentation on the Amazon continental margin: a model, Geological Society of America Bulletin, 86, 610-614, 1975.
Missiaen, L., Pichat, S., Waelbroeck, C., Douville, E., Bordier, L., Dapoigny, A., Thil, F., Foliot, L., and Wacker, L.: Downcore variations of sedimentary detrital (238U/232Th) ratio: implications on the use of 230Thxs and 231Paxs to reconstruct sediment flux and ocean circulation, Geochemistry, Geophysics, Geosystems, 10.1029/2017GC007410, in press.
Mulitza, S., Chiessi, C. M., Schefuß, E., Lippold, J., Wichmann, D., Antz, B., Mackensen, A., Paul, A., Prange, M., and Rehfeld, K.: Synchronous and proportional deglacial changes in Atlantic Meridional Overturning and northeast Brazilian precipitation, Paleoceanography, 2017.
Rasmussen, S. O., Bigler, M., Blockley, S. P., Blunier, T., Buchardt, S. L., Clausen, H. B., Cvijanovic, I., Dahl-Jensen, D., Johnsen, S. J., and Fischer, H.: A stratigraphic framework for abrupt climatic changes during the Last Glacial period based on three synchronized Greenland ice-core records: refining and extending the INTIMATE event stratigraphy, Quaternary Science Reviews, 106, 14-28, 2014.
Reimer, P., Bard, E., Bayliss, A., Beck, J. W., Blackwell, P. G., Bronk Ramsey, C., Buck, C. E., Cheng, H., Edwards, R. L., Friedrich, M., Grootes, P. M., Guilderson, T. P., Haflidason, H., and ... IntCal13 and Marine13 radiocarbon age calibration curves 0–50,000 years cal BP, Radiocarbon, 55, 1869–1887, 2013.

Rhein, M., Kieke, D., and Steinfeldt, R.: Advection of North Atlantic Deep Water from the Labrador Sea to the southern hemisphere, Journal of Geophysical Research: Oceans, 120, 2471-2487, 2015.
Rühlemann, C., Frank, M., Hale, W., Mangini, A., Mulitza, S., Müller, P., and Wefer, G.: Late Quaternary productivity changes in the western equatorial Atlantic: Evidence from 230Th-normalized carbonate and organic carbon accumulation rates, Marine Geology, 135, 127-152, 1996.
Schmittner, A., Bostock, H. C., Cartapanis, O., Curry, W. B., Filipsson, H. L., Galbraith, E. D., Gottschalk, J., Herguera, J. C., Hoogakker, B., Jaccard, S. L., Lisiecki, L. E., Lund, D. C., Martínez-Méndez, G., Lynch-Stieglitz, J., Mackensen, A., Michel, E., Mix, A. C., Oppo, D. W., Peterson, C. D., Repschläger, J., Sikes, E. L., Spero, H. J., and Waelbroeck, C.: Calibration of the carbon isotope composition (δ13C) of benthic foraminifera, Paleoceanography, 32, doi:10.1002/2016PA003072, 10.1002/2016PA003072, 2017.
Scholten, J., Botz, R., Paetsch, H., and Stoffers, P.: 230Thex flux into Norwegian-Greenland Sea sediments: Evidence for lateral sediment transport during the past 300,000 years, Earth and planetary science letters, 121, 111-124, 1994.
Schott, F. A., Dengler, M., Brandt, P., Affler, K., Fischer, J., Bourles, B., Gouriou, Y., Molinari, R. L., and Rhein, M.: The zonal currents and transports at 35 W in the tropical Atlantic, Geophysical Research Letters, 30, 2003.
Sepulcre, S., Durand, N., and Bard, E.: Large 14C age offsets between the fine fraction and coexisting planktonic foraminifera in shallow Caribbean sediments, Quaternary Geochronology, 38, 61-74, 2017.
Taylor, S., and McLennan, S.: The continental crust: its composition and evolution, Oxford: Blackwell Press, 312 pp., 1985.
Thomas, A. L., Henderson, G. M., and Robinson, L. F.: Interpretation of the 231Pa/230Th paleocirculation proxy: New water-column measurements from the southwest Indian Ocean, Earth and Planetary Science Letters, 241, 493-504, 2006.
Thomson, J., Colley, S., Anderson, R., Cook, G., MacKenzie, A., and Harkness, D.: Holocene sediment fluxes in the northeast Atlantic from 230Thexcess and radiocarbon measurements, Paleoceanography, 8, 631-650, 1993.
Thornalley, D. J. R., Barker, S., Broecker, W. S., Elderfield, H., and McCave, I. N.: The Deglacial Evolution of North Atlantic Deep Convection, Science, 331, 202-205, 2011.
Torrence, C., and Compo, G. P.: A practical guide to wavelet analysis, Bulletin of the American Meteorological society, 79, 61-78, 1998.
Torrence, C., and Webster, P. J.: Interdecadal changes in the ENSO–monsoon system, Journal of Climate, 12, 2679-2690, 1999.
Vazquez Riveiros, N., Waelbroeck, C., Roche, D. M., Moreira, S., Burckel, P., Dewilde, F., Skinner, L., Böhm, E., Arz, H. W., and Dokken, T.: Northern origin of western tropical Atlantic deep waters during Heinrich Stadials, submitted.
Vidal, L., Labeyrie, L., Cortijo, E., Arnold, M., Duplessy, J. C., Michel, E., Becqué, S., and van Weering, T. C. E.: Evidence for changes in the North Atlantic Deep Water linked to meltwater surges during the Heinrich events, Earth and Planetary Science Letters, 146, 13-26, 1997.
Waelbroeck, C., Duplessy, J.-C., Michel, E., Labeyrie, L., Paillard, D., and Duprat, J.: The timing of the last deglaciation in North Atlantic climate records, Nature, 412, 724-727, 2001.
Weltje, G. J., and Tjallingii, R.: Calibration of XRF core scanners for quantitative geochemical logging of sediment cores: theory and application, Earth and Planetary Science Letters, 274, 423-438, 2008.
Wheatcroft, R. A.: Experimental tests for particule size-dependent bioturbation in the deep ocean, Limnol. Oceanogr., 37, 90-104, 1992.
Wilson, K. E., Maslin, M. A., and Burns, S. J.: Evidence for a prolonged retroflection of the North Brazil Current during glacial stages, Palaeogeography, Palaeoclimatology, Palaeoecology, 301, 86-96, 2011.
Yu, E.-F., François, R., and Bacon, M.: Similar rates of modern and last-glacial ocean thermohaline circulation inferred from radiochemical data, Nature, 379, 689-694, 1996.
Zahn, R., Winn, K., and Sarnthein, M.: Benthic foraminiferal δ13C and accumulation rates of organic carbon: Uvigerina peregrina group and Cibicidoides wuellerstorfi, Paleoceanography, 1, 27-42, 1986.
Zhang, D., Msadek, R., McPhaden, M. J., and Delworth, T.: Multidecadal variability of the North Brazil Current and its connection to the Atlantic meridional overturning circulation, Journal of Geophysical Research: Oceans, 116, 2011.

Zhang, Y., Chiessi, C. M., Mulitza, S., Zabel, M., Trindade, R. I., Hollanda, M. H. B., Dantas, E. L., Govin, A., Tiedemann, R., and Wefer, G.: Origin of increased terrigenous supply to the NE South American continental margin during Heinrich Stadial 1 and the Younger Dryas, Earth and Planetary Science Letters, 432, 493-500, 2015.

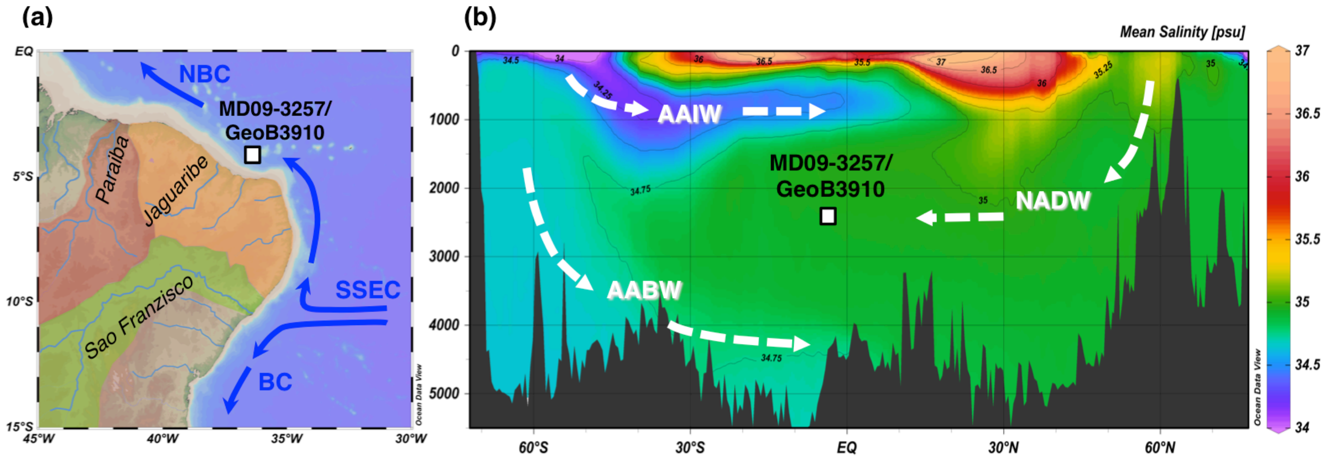

Figure 1: (a) Map showing the position of the main Brazilian rivers and surface currents that could influence the terrigenous input at the study site indicated by a white square. The orange area represents the catchment area of the local rivers directly delivering sediments to our study site, and the green area represents the catchment area of the Sao Franzisco River (Milliman et al., 1975). **(b)** Salinity section showing the core site and main water masses in the modern Atlantic Ocean.

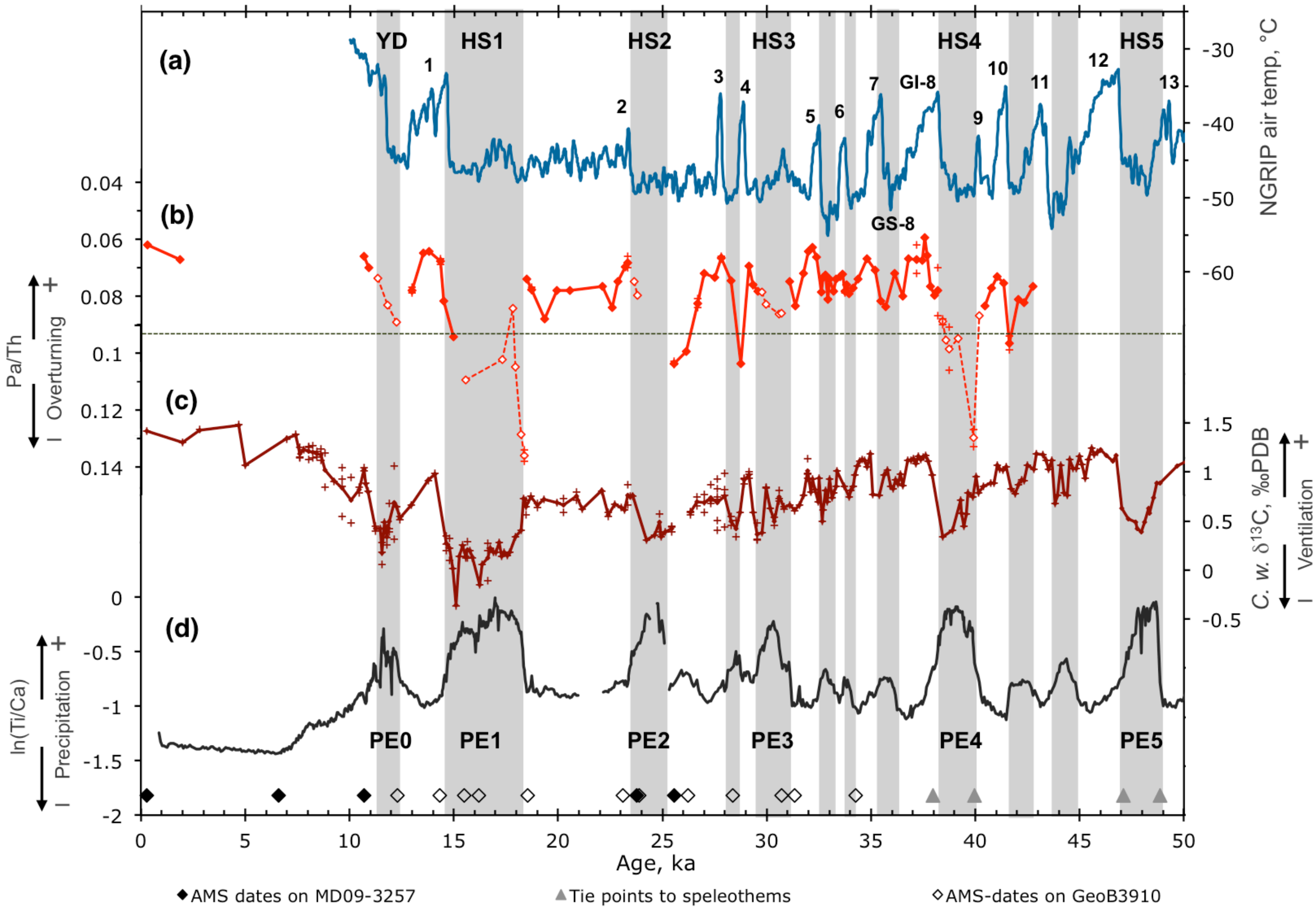

Figure 2: MD09-3257 Pa/Th, ln(Ti/Ca) and composite *C. wuellerstorfi* $\delta^{13}C$ ($\delta^{13}C_{Cw}$) records versus MD09-3257 age scale, independent from NGRIP age scale. **(a)** NGRIP air temperature versus GICC05 age scale (Kindler et al., 2014), transposed from ky b2k to ka. Greenland interstadials are numbered according to (Rasmussen et al., 2014). To avoid over-crowding of the figure, Greenland stadials (GS) and interstadials (GI) are explicitly named only in the case of GS-8 and GI-8. **(b)** Core MD09-3257 Pa/Th record. Empty symbols denote data points that may be affected by terrigenous fluxes and should be interpreted with caution; crosses denote replicate measurements; the red line connects average values (filled symbols). Pa/Th could not be measured over the first half of PE2 because of the occurrence of two small sand layers (Burckel et al., 2015). **(c)** Core MD09-3257 and GeoB3910-2 composite $\delta^{13}C_{Cw}$ record (Vazquez Riveiros et al., submitted); crosses denote replicate measurements. **(d)** MD09-3257 ln(Ti/Ca). Diamonds above the X-axis indicate calibrated radiocarbon dates in MD09-3257 (filled symbols) and GeoB3910-2 (empty symbols). Triangles indicate alignment tie points to South American speleothem $\delta^{18}O$ (Vazquez Riveiros et al., submitted). Grey bands delineate precipitation events recorded in MD09-3257 ln(Ti/Ca).

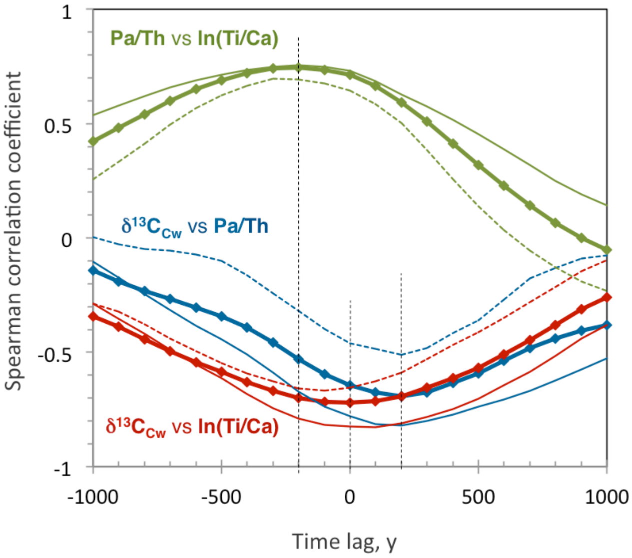

Figure 3: Spearman correlation coefficient of $\delta^{13}C_{Cw}$ vs Pa/Th (blue curves), of $\delta^{13}C_{Cw}$ vs ln(Ti/Ca) (red curves), and of Pa/Th vs ln(Ti/Ca) (green curves), as a function of the time lag. A positive time lag means that series 1 lags series 2 (e.g. $\delta^{13}C_{Cw}$ lags Pa/Th); a negative time lag means that series 1 leads series 2 (e.g. Pa/Th leads ln(Ti/Ca)). Bold lines correspond to the calculation over the entire time interval 10.6-42.6 ka, thin lines to the calculation over 10.6-26.6 ka, and thin dashed lines to the calculation over 26.6-42.6 ka. Vertical dashed lines indicate the time lags corresponding to the maximum correlation coefficients for the three pairs of series over the entire time interval.

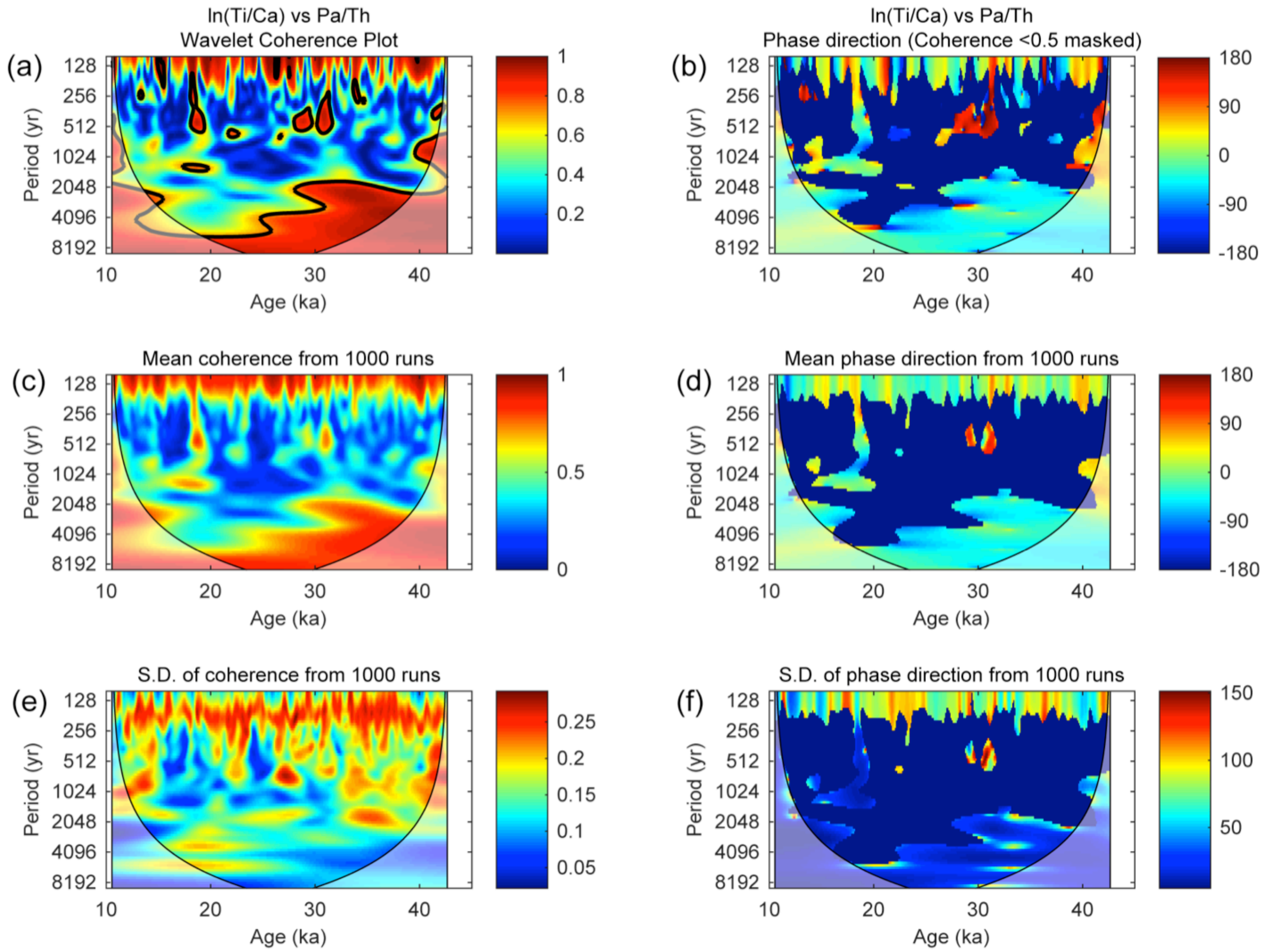

Figure 4: Cross-wavelet transform of MD09-3257 ln(Ti/Ca) versus Pa/Th. **(a, b)** Wavelet coherence and phase direction computed using (Grinsted et al., 2004) software. The thick contour line corresponds to the 95% confidence level against red noise. Phase direction is computed only for coherences higher than 0.5. **(c, d)** Mean coherence and phase direction computed out of 1000 Monte Carlo simulations. **(e, f)** Standard deviation around the mean coherence and phase direction computed out of these 1000 Monte Carlo simulations.

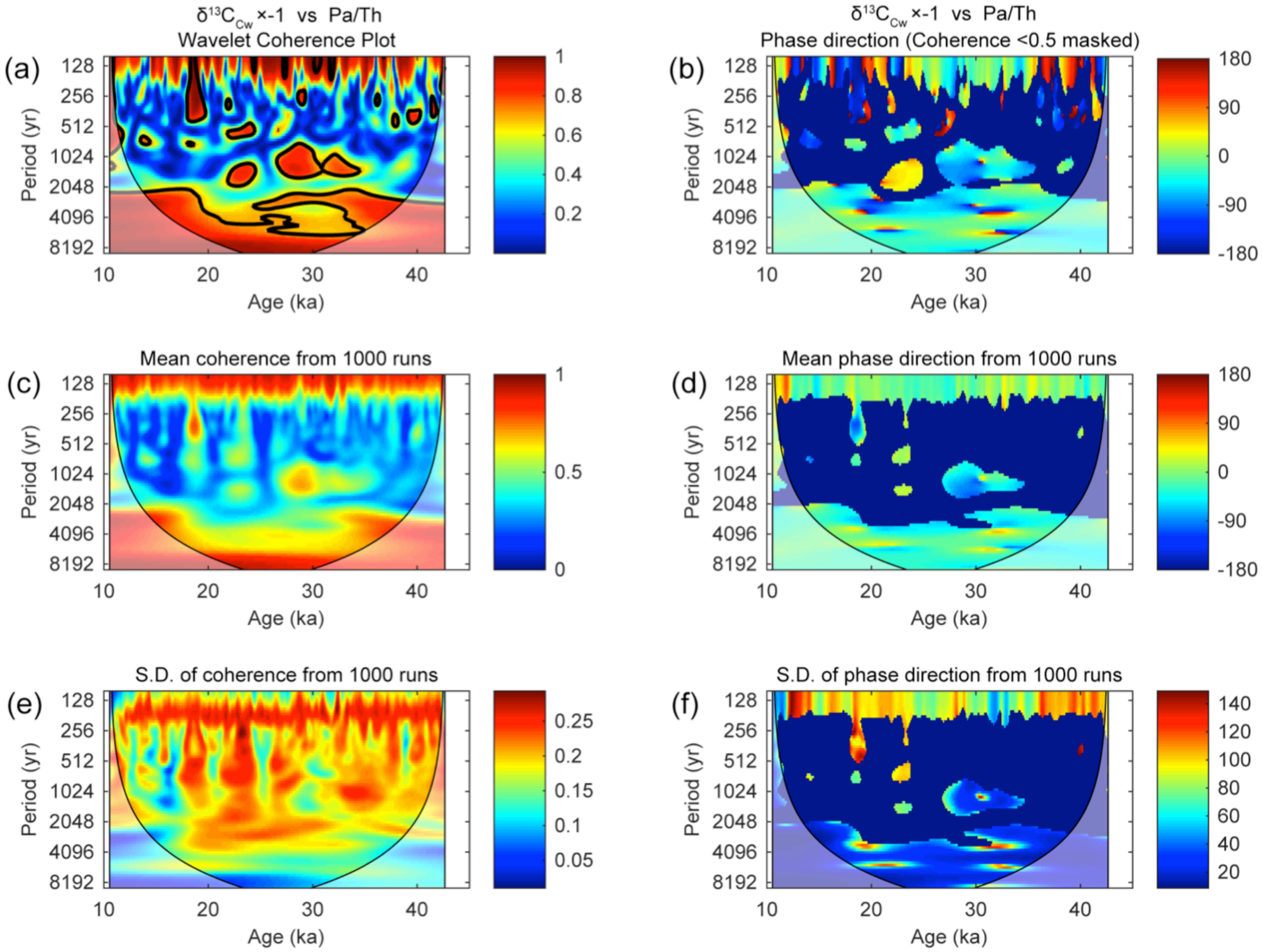

Figure 5: Cross-wavelet transform of $\delta^{13}C_{Cw}$ composite record versus MD09-3257 Pa/Th. $\delta^{13}C_{Cw}$ values have been multiplied by (-1) to allow a straightforward reading of the relative phase between a decrease in $\delta^{13}C$ and an increase in Pa/Th. **(a-f)** as in Fig. 4.

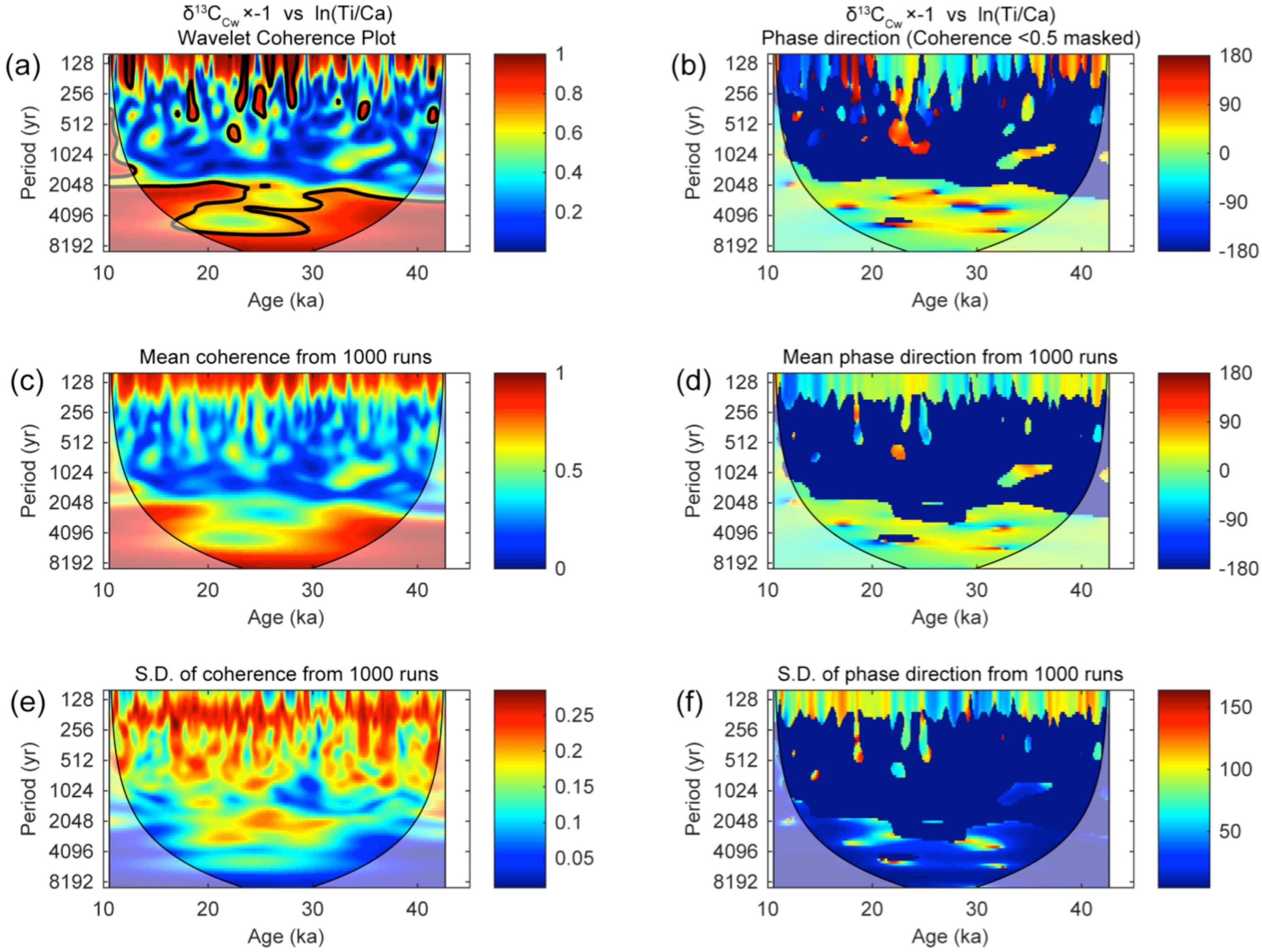

Figure 6: Cross-wavelet transform of $\delta^{13}C_{Cw}$ composite record versus MD09-3257 ln(Ti/Ca). $\delta^{13}C_{Cw}$ values have been multiplied by (-1) to allow a straightforward reading of the relative phase between a decrease in $\delta^{13}C$ and an increase in ln(Ti/Ca). **(a-f)** as in Fig. 4 and 5.

Table 1. Relative phases over regions of the cross-wavelet graphs corresponding to coherences > 0.5

	Time interval	Period range	Periodicity	Phase, deg	1σ, deg	Phase, y	1σ, y	Comment
ln(Ti/Ca) vs Pa/Th (Fig. 4)	28-40 ka*	1000-3000	**2000**	**-46.7**	**25.2**	**-259**	**140**	**Pa/Th leads ln(Ti/Ca)**
	15-40 ka*	4000-6000	**5000**	**-45.4**	**24.8**	**-631**	**345**	**Pa/Th leads ln(Ti/Ca)**
$\delta^{13}C_{Cw}$ vs Pa/Th (Fig. 5)	28-40 ka	1000-3000	**2000**	**-50.2**	**39.7**	**-279**	**244**	**Pa/Th leads $\delta^{13}C_{Cw}$**
	15-40 ka	4000-6000	5000	-14.1	37.1	-196	525	not significant
$\delta^{13}C_{Cw}$ vs ln(Ti/Ca) (Fig. 6)	28-40 ka	1000-3000	2000	17	24.3	94	171	not significant
	15-40 ka	4000-6000	5000	10.8	42.9	150	606	not significant

*within these time intervals, only results from the unshaded region of the wavelet graphs are taken into account.